**NUCLEAR ENERGY RESEARCH INITIATIVE (NERI)**
**QUARTERLY PROGRESS REPORT**

# Engineering and Physics Optimization of Breed and Burn Fast Reactor Systems

**Quarterly Report**
**October 1, 2004—December 31, 2004**

**January 31, 2005**

**Lead Organization: Massachusetts Institute of Technology**
**77 Massachusetts Avenue, Cambridge, MA 02139**

**Project (Grant No. DE-FG07-02SF22608)**
**Project No. 2002-005**

**LEAD ORGANIZATION:**

| Principal Investigator: | Other Collaborators: |
|---|---|
| Michael Driscoll | Kenneth R. Czerwinski (UNLV) |
| Telephone: (617) 253-4219 | Pavel Hejzlar (MIT) |
| Email: mickeyd@mit.edu | Pradip Saha (MIT) |

**COLLABORATING ORGANIZATIONS:**

**Idaho National Engineering and Environmental Laboratory**
**PO Box 1625**
**Idaho Falls, ID 83415**

| Co-Principal Investigator: | Other Collaborators: |
|---|---|
| Kevan D. Weaver | James Parry |
| Telephone: (208) 526-0321 | Theron D. Marshall |
| Email: weavkd@inel.gov | Cliff B. Davis |

**Argonne National Laboratory – West**
**PO Box 2528**
**Idaho Falls, ID 83401**

| Co-Principal Investigator: | Other Collaborators: |
|---|---|
| Mitchell K. Meyer | Daniel M. Wachs |
| Telephone: (208) 533-7461 | |
| Email: mitchell.meyer@anl.gov | |

**DOE-HQ Contact**

| | |
|---|---|
| Buzz Savage | Route Symbol: NE-20, Bldg: GTN |
| Physical Scientist | 1000 Independence Ave. SW |
| U.S. Department of Energy | Washington, DC 20585-1290 |

## Table of Contents


Table of Contents ..... 1
List of Tables ..... 2
List of Figures ..... 2
1. Technical Narrative ..... 3
General ..... 3
Overview ..... 3
Task A Core Physics and Fuel Cycle ..... 6
Tube-In-Duct Reactor Physics Analysis ..... 6
Description of the Work ..... 7
Results ..... 7
Conclusions ..... 9
References ..... 9
Doppler Reactivity Feedback (Pin Core) ..... 11
Fuel Cycle Economics (Pin Core) ..... 12
Fission Product Buildup and Spent Fuel Reprocessing (Pin Core) ..... 13
Core Physics INEEL ..... 14
Core Physics ..... 14
Future Work ..... 14
B&B GFR Fuel Cycle ..... 15
Fuel Cycle Cost ..... 15
Cost of N-15 ..... 16
Tasks A.4 and A.5 ..... 18
Fuel Processing and Reuse ..... 18
Kinetic Evaluation of Fission Element Removal by CARDIO ..... 19
Tasks B and C Core Thermal Hydraulics and Plant Design ..... 22
Task B/C.1 Thermal-Hydraulic Modeling at INEEL ..... 22
Task C Plant Design ..... 26
Shutdown Heat Removal ..... 26
Task D Fuel Design ..... 27
D.1 Task Status and Significant Results ..... 27
Future Work ..... 28
Appendix A Indirect He-to-S-$CO_2$ Brayton vs. He-to-Rankine Cycle Comparison ..... 29
Appendix B An Advanced Vented Fuel Assembly Design for GFR Applications ..... 32
Appendix C Numerical Benchmark Specifications for TID Fuel Assembly ..... 36
Appendix D Heatric™ PCHE With 2:1 Channel Ratio ..... 46
Appendix E GFR Project Publications ..... 47
Task Flowchart ..... 53
Milestone Status Table ..... 54
Financial Reports ..... 55
6893961 Distribution List—Neri B&B ..... 58

## List of Tables


Table 0.1 Reference Design Features of Breed and Burn GFR Concept ..... 5
Table A.1 Doppler Reactivity Feedback Coefficient Results ..... 11
Table A.2 Direct Front End Costs of B&B Fueling Options ..... 15
Table A-C.1 Parameters for a Numerical Benchmark of T&H Models ..... 37


## List of Figures


Fig. A.1 TID Conceptual Diagram ..... 6
Fig. A.2 BOC Infinite Reactivity Assessment for TID Fuel ..... 8
Fig. A.3 Burnup Histories for Various Fuel Volume Fractions ..... 9
Fig. A.4 Comparison of 238U Fission Cross Section Libraries ..... 12
Fig. A.5 Fuel Cycle Cost as a Function of HEN Cost ..... 13
Fig. A.6 Buildup of Dominant Fission Products in B&B Fuel ..... 14
Fig. A.7 Sm Removal vs. Time ..... 19
Fig. A.8 Microprobe of ZrN and CeN Ceramics ..... 21
Fig. B/C.1 Initial ATHENA Model of the Containment Building ..... 23
Fig. B/C.2 ATHENA Model of Containment Building and RCC ..... 24
Fig. B/C.3 Four Volume Configuration for the Containment Building ..... 24
Fig. B/C.4 Schematic of ATHENA Model for GFR-He Design with $CO_2$ Injection System for LOCA ..... 25
Fig. A-A.1 Intermediate Heat Exchanger (IHX) Temperature Profiles ..... 31
Fig. A-B.1 TID Assembly Vertical Cross-Sectional View ..... 34
Fig. A-B.2 Advanced TID Coolant Tube Configuration ..... 35
Fig. A-C.1 Horizontal Cross-Section of Unit Cell ..... 39
Fig. A-C.2 Vertical Cross-Section of Unit Cell ..... 40
Fig. A-C.3 Conductivity Versus Temperature for ODS MA956 ..... 41

# NERI QUARTERLY PROGRESS REPORT

"Engineering and Physics Optimization of Breed and Burn Fast Reactor Systems"

Project No. 2002-005

Period: October-December 2004

## 1. Technical Narrative

### General

This project is organized under four major tasks (each of which has two or more subtasks) with contributions among the three collaborating organizations (MIT, INEEL and ANL-West):

Task A: Core Physics and Fuel Cycle
Task B: Core Thermal Hydraulics
Task C: Plant Design
Task D: Fuel Design

The lead PI, Michael J. Driscoll, has consolidated and summarized the technical progress submissions provided by the contributing investigators from all sites, under the above principal task headings.

The following paper was presented at the November 14-18, 2004 ANS Winter Meeting:

P. Yarsky, M. J. Driscoll, P. Hejzlar, "Design of a Once-Through Breed and Burn GFR", Trans. Am. Nucl. Soc., Vol. 91, Nov. 2004

### Overview

Two important decisions have been made as the result of system integration studies over the past six months.

1. The reference power cycle has been chanced from indirect Supercritical $CO_2$ Brayton to (indirect) Rankine.
2. The reference core assembly has been changed from pin-type to tube-in-duct type.

The first decision follows from the nature of the S-$CO_2$ cycle, which optimizes out at about 400°C core inlet temperature and 150°C core coolant temperature rise. This results in very high primary system circulator power consumption, made worse by the need for high fuel volume fraction (low coolant fraction) in B&B cores. In contrast core $\Delta T_c$ can be much larger when a Rankine cycle is employed. For example, the Dungeness and Hartlepool AGRs in the

UK have $\Delta T_c = 395°C$ with efficiencies of 44.4% gross and 41.7% net. Appendix A summarizes these considerations in a more quantitative fashion.

The second decision has been mentioned in earlier reports. It is related to the first in that lower core pressure drops and fuel temperatures are an inherent characteristic of tube-in-duct assemblies. Appendix B is a draft technical note on this subject submitted for the June 2005 ANS meeting and associated ANS transactions.

A contributing factor motivating these changes has been the desire to qualify a core for B&B service based on the use of UC fuel in place of the UN-15 we have focused on up until recently. UC is considerably less expensive and is far more proven in terms of experience in fast reactor (LMR) applications. However, it is neutronically inferior to UN-15, which strengthens the emphasis on high fuel volume fraction.

As part of the effort to qualify the new assembly design we have also considered definition of a thermal-hydraulic benchmark, which will ensure that MIT, INEEL and ANL West have a common starting point for their further investigations. The benchmark is described in Appendix C.

It is worth noting that for non-Breed & Burn applications, the S-$CO_2$ cycle can still be a competitive indirect cycle option even for gas-to gas concepts. As noted in Appendix D, Heatric™ PCHE Type IHX units can employ a 2:1 ratio of primary to secondary channels to significantly reduce pressure drop. More importantly, higher core coolant fractions can be employed and if one returns to conventional breeder designs using fertile blankets, an even more open core is practicable because the internal conversion ratio no longer need be increased to near unity.

Table O.1 summarizes the current status of key design features for the B&B GFR core and its supporting balance of plant.

**Table 0.1 Reference Design Features of Breed and Burn GFR Concept**

| **Core** | | **Comments:** |
|---|---|---|
| Fuel: | UC or<br>UN-15 | $UO_2$ not viable neutronically<br>Reaction of UN and UC with $CO_2$ precludes its use as coolant |
| Clad: | ODS | ODS may be able to resist creep adequately up to ≈700ºC |
| Configuration: | Tube-in-Duct; Vented; Orificed | Lower fuel T at increased fuel fraction; venting eliminates ΔP across clad |
| Coolant: | He@10 MPa, Indirect Cycle;<br>Core ΔTc = 380°C,<br>Exit T≈600°C | He is inert chemically, used in thermal HTGRs |
| Thermal-Hydraulics | AXIAL Peaking Factor = 1.45<br>Radial Peaking, Factor = 1.77,<br>Power Density 130 W/cc | Orificing reduces circulator power by factor of ≈2 |
| Burnup | 150 MWd/kg Over 18 EFPY | ρ > 0 @ ≈ 20 MWd/kg<br>ρ peaks @ ≈ 80 MWd/kg |
| **Plant** | | |
| Power Cycle: | Rankine<br>2400 $MW_{th}$ | Allows ≈ 380°C ΔTc across core, which reduces coolant flow rate, hence circulator power |
| Reactor Vessel: | Prestressed Cast Iron Vessel (PCIV)<br>or<br>Prestressed Concrete Reactor Vessel (PCRV) | PCIV is modular, more T resistant than concrete, accommodates large core, envelopes IHX and shutdown loops<br>PCRV is proven in GCR service (but at lower P) |
| Shutdown Cooling System: (combined shutdown & emergency) | • 3 x 50% capable forced convection loops<br>• Water-boiler heat sink | PRA-guided design supports this selection (basically same No. loops as GCFRs of the 1970's)<br>Natural convection alone suffices if P≥12 atm (5 if $CO_2$ injected) |
| Containment: | PWR type sized to keep post-LOCA pressure ≤ 5 atm | Combined with $CO_2$ injection this permits decay heat removal solely by natural convection |

**Task A Core Physics and Fuel Cycle**

**Tube-In-Duct Reactor Physics Analysis**

(Paper submitted for June 2005 ANS meeting)

**Contributors: P. Yarsky, M.A. Pope, M.J. Driscoll, P. Hejzlar (MIT)**

For a reactor to operate in the Breed and Burn (B&B) mode, the core must have a large heavy metal loading to sustain criticality through cycle lengths allowable by structural material performance. With a large heavy metal loading in each assembly, and a discharge burnup greater than 150 MWD/kgHM it is essential, from an economic perspective, for the core to operate at high power density. The Tube-in-Duct (TID) fuel assembly concept has evolved over several years to meet the competing design requirements for service in a B&B GFR. The purpose of the current NERI funded work is to study the impacts of fuel/coolant volume fraction on the neutronic performance of such a fuel assembly.

The TID fuel assembly utilizes hexagonal pitch coolant tubes surrounded by a vibrationally compacted (VIPAC) UC or $U^{15}N$ fuel inside a vented assembly duct.[6] The fuel volume fraction in the TID fuel assembly is higher than that achievable with a standard pin-type assembly without compromising the peak clad temperature. The design also eliminates the need for pin spacers which helps to minimize core pressure drop.

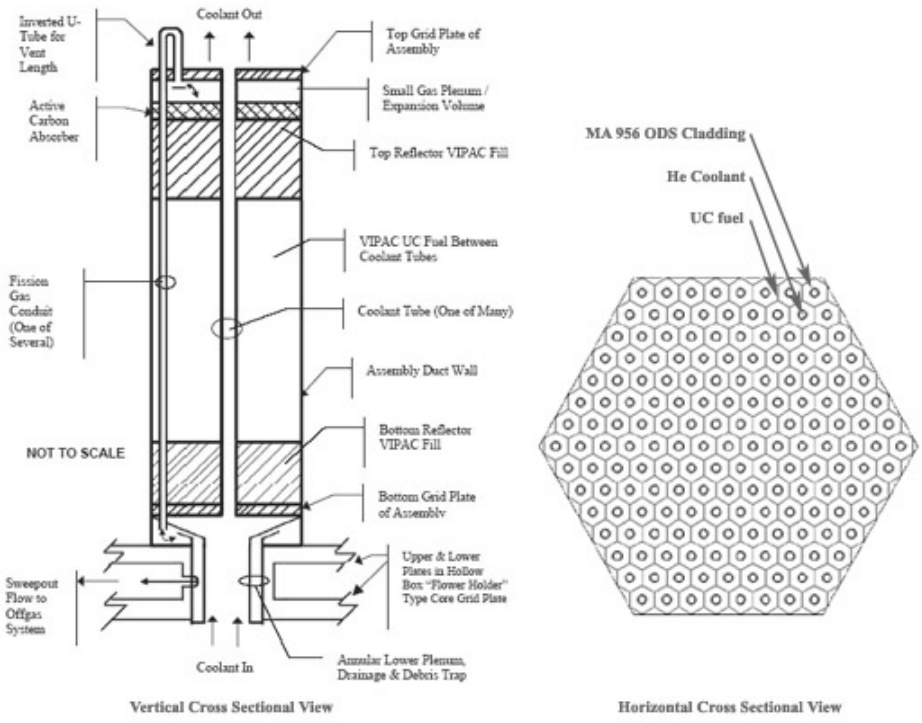


**Fig. A.1: TID Conceptual Diagram**

MCNP4c3 and ORIGEN2.2 were used to evaluate BOL eigenvalues as well as the burnup behavior of the TID fuel assembly for various enrichments and coolant channel dimensions. The purpose of this work is to enumerate the trade offs between thermal hydraulic performance of a TID core and neutronic performance.

**Description of the Work**

An MCNP model was created for a UC fueled, MA956 ODS steel clad, helium cooled TID fuel assembly. The assembly had mirror boundary conditions on the edge of the ODS duct radially, and allowed for neutron leakage through the upper and lower axial $Zr_3Si_2$ reflectors. MCNP4c3 was coupled with ORIGEN2.2 using a code developed at MIT called MCODE.[7] The reference assembly model has a flat-to-flat distance of 13.3 cm,169 coolant channels, and 8 axial fuel zones.

The BOL assembly eigenvalue was calculated for enrichments of 5 a/o and 10 a/o $^{235}U$. The coolant channel inner radius was varied between 0.15 cm and 0.45 cm. For coolant channel radii of 0.15 cm, 0.30 cm, and 0.40 cm MCODE was used to simulate the burnup of the assembly to 300 MWD/kgHM. These cases were evaluated solely to compare the physics performance; in practice one would vary pin pitch at constant coolant tube diameter.

**Results**

Figure 1.5 shows a plot based on BOC assembly reactivity calculations. The reactivity is plotted against the ratio of the theoretical heavy metal density to the homogenous heavy metal density (the heavy metal density smeared over the whole assembly volume). The curves clearly illustrate the dependence of the reactivity on the heavy metal density. As the two BOC curves are nearly linear, one can easily predict the BOC reactivity based on the initial enrichment using a linear model.

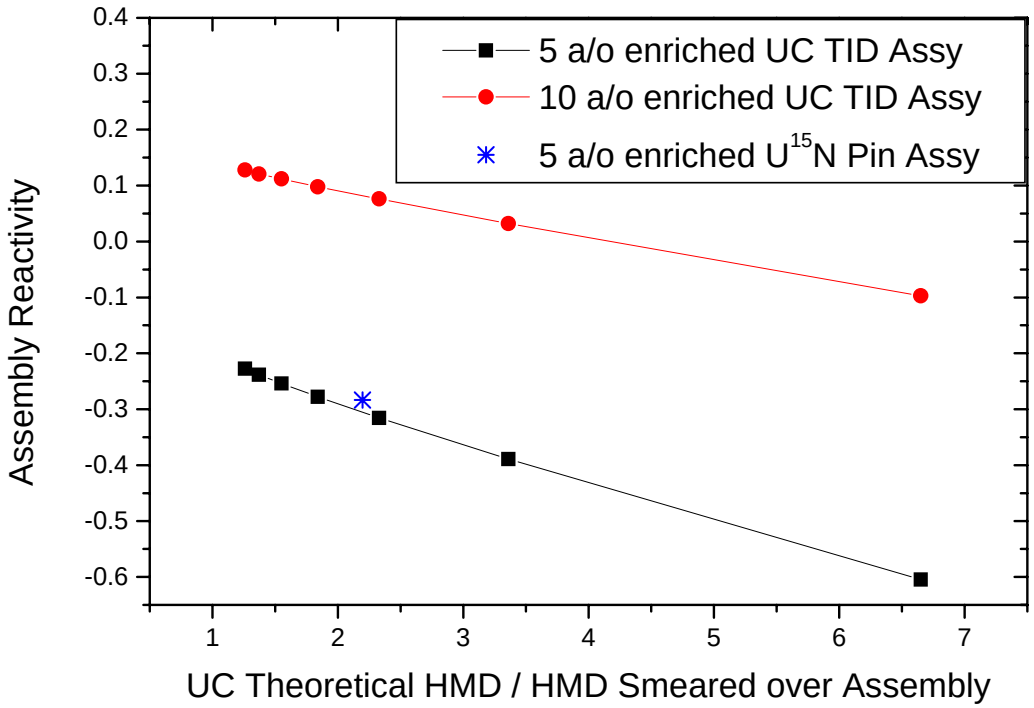


**Fig. A.2: BOC Infinite Reactivity Assessment for TID Fuel**

The next set of analyses were carried out on several example cases to illustrate the behavior of the 5a/o enriched fuel during burnup. As Figure 1.6 illustrates, increasing the volume fraction much larger than 60% only yields a reactivity benefit on the order of 200 pcm. Additionally, it is worth noting that the reactivity difference between the two cases is fairly constant throughout burnup. Therefore it is possible to predict the burnup trend for the TID fuel based on the coolant or fuel volume fraction and BOC reactivity. Additionally, a $U^{15}N$ fueled pin assembly is also shown to illustrate the competitiveness of the TID concept in terms of meeting the requirements for B&B operation.

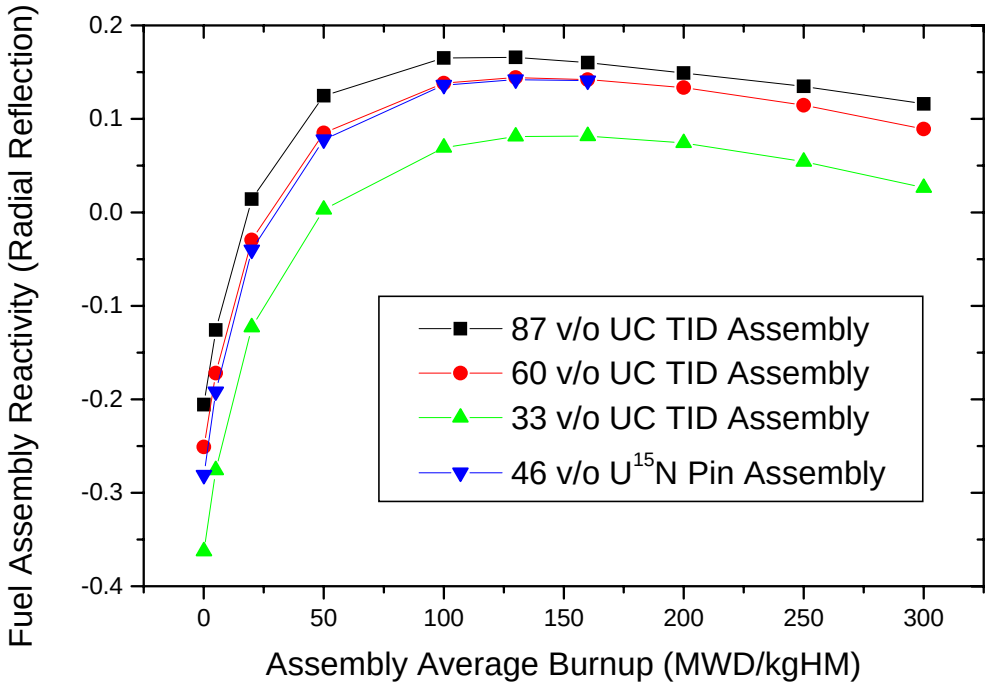


**Fig. A.3: Burnup Histories for Various Fuel Volume Fractions**

The $U^{15}N$ fueled pin assembly used for the former comparison has been shown to enable B&B operation with a discharge burnup of 150 MWD/kgHM.[8] To achieve B&B operation with UC, the results of these analyses show that ~60 v/o fuel will be required with the TID assembly to avoid the need for spent fuel recycle.

## Conclusions

Parametric physics analyses of the TID fuel assembly, when coupled with thermal hydraulic models of the core will allow for rapid assessment of the tradeoffs between thermal and neutronic performance, thus accelerating the optimization of a core with this type of fuel.

## References

1. Inoue, M., Ono, K., Fujioka, T., Sato, K., Asaga, T., *Feasibility Study on Nitrogen-15 Enrichment and Recycling System for Innovative FR Cycle System with Nitride Fuel,* ICONE10-22622, Arlington, Virginia, USA, (April 2002)
2. Suzuki, Y., Ogawa, T., Arai, Y., Mukaiyama, T. *Recent Progress of Research on Nitride Fuel Cycle in JAERI*, Fifth OECD/NEA Information Exchange Meeting on Actinide and Fission Product Partitioning and Transmutation, 3-3, Jeju, Republic of Korea (October 2002)

3. Yarsky, P., Driscoll, M.J, Hejzlar, P., *Use of Minimally Processed Fast Reactor Fuel in Light Water Reactors*, Trans. Am. Nucl. Soc., Vol. 90 (June 2004).
4. Gas-Cooled Fast Breeder Reactor Preliminary Safety Information Documment – Amendment 10, General Atomic Company GA-10298 (September 1980)
5. Todreas, N., Kazimi, M.: Nuclear Systems I Thermal Hydraulic Fundamentals, Taylor and Francis. New York, 1993.
6. Pope, M.A., Yarsky, P., Driscoll, M.J, Hejzlar, P., *An Advanced Vented Fuel Assembly for GFR Applications* ,Trans. Am. Nucl. Soc. (June 2005).
7. Xu, Z., P. Hejzlar, M.J. Driscoll, M.S. Kazimi, "An Improved MCNP-ORIGEN Depletion Program (MCODE) and its Verification for High-Burnup Applications,*International Conference on the New Frontiers of Nuclear Technology: Reactor Physics, Safety and High-Performance Computing (PHYSOR 2002),* Seoul, Korea, October 7-10, 2002.
8. Yarsky, P., Driscoll, M.J., Hejzlar, P. *Design of a Once-through B&B GFR,* Trans. Am. Nucl. Soc., Vol. 91 (November 2004).

**Doppler Reactivity Feedback (Pin Core)**

The Doppler Coefficient ($\alpha$, $\Delta\rho$ per $^{o}C$) of the B&B GFR was investigated using EOC Equilibrium core MCNP models. Prebroadened ENDFBVI and JEF2.2 libraries were available. Two points were evaluated using each library set. The following libraries were used: ENDFBVI at 300K and 900K as well as JEF2.2 at 300K and 1000K. A $T^{-1/2}$ dependence for the Doppler coefficient was assumed to calculate the point value at 900K.

The following table summarizes the results of the full core as well as a unit cell – fuel pin analysis.

**Table A.1 Doppler Reactivity Feedback Coefficient Results**

| | $\alpha$D (900K) | | std-dev |
|---|---|---|---|
| Full Core | | | |
| ENDFBVI | -0.83 | pcm/oC | 0.07 |
| JEF2.2 | -0.29 | pcm/oC | 0.04 |
| Coarse Pin | | | |
| ENDFBVI | -0.93 | pcm/oC | 0.33 |
| JEF2.2 | -0.55 | pcm/oC | 0.24 |
| Fine Pin | | | |
| ENDFBVI | -0.86 | pcm/oC | 0.01 |
| JEF2.2 | -0.91 | pcm/oC | 0.01 |

It was found that the ENDFBVI library results for the full core model were much larger in magnitude than those predicted by the JEF2.2 libraries. To investigate the difference, a simple, representative unit cell model was created such that in reasonable run times (on the order of days) MCNP could generate eigenvalues with sufficiently numerous neutron histories, hence small enough statistical errors to compare the results.

The designators "coarse" and "fine" refer to the number of neutron histories. As one can see, when the errors remain large, the JEF2.2 continues to underpredict the Doppler coefficient. The two results converged, but only once the errors in the eigenvalue were exceptionally small (std-dev ~ 0.00005). The JEF2.2 libraries consistently predicted a smaller eigenvalue than the ENDFBVI libraries and yielded, at the end a larger Doppler coefficient. This is possibly due to the treatment of the $^{238}U$ fission cross section, which, in the JEF2.2 libraries, has a "step" near the energy range where the neutron flux spectrum is peaked (~ 150 keV): see Figure A.4.

As the ENDFBVI libraries predicted consistent results between the representative fuel pin and the core, and did not show as great a sensitivity to the precision of the calculation, this is the cross section set of choice for doing further analyses. However, the strong consistency in the Doppler coefficient between the pin-cell and full core models indicates that unit cell analyses can be used to estimate the Doppler coefficient accurately enough for the present purpose.

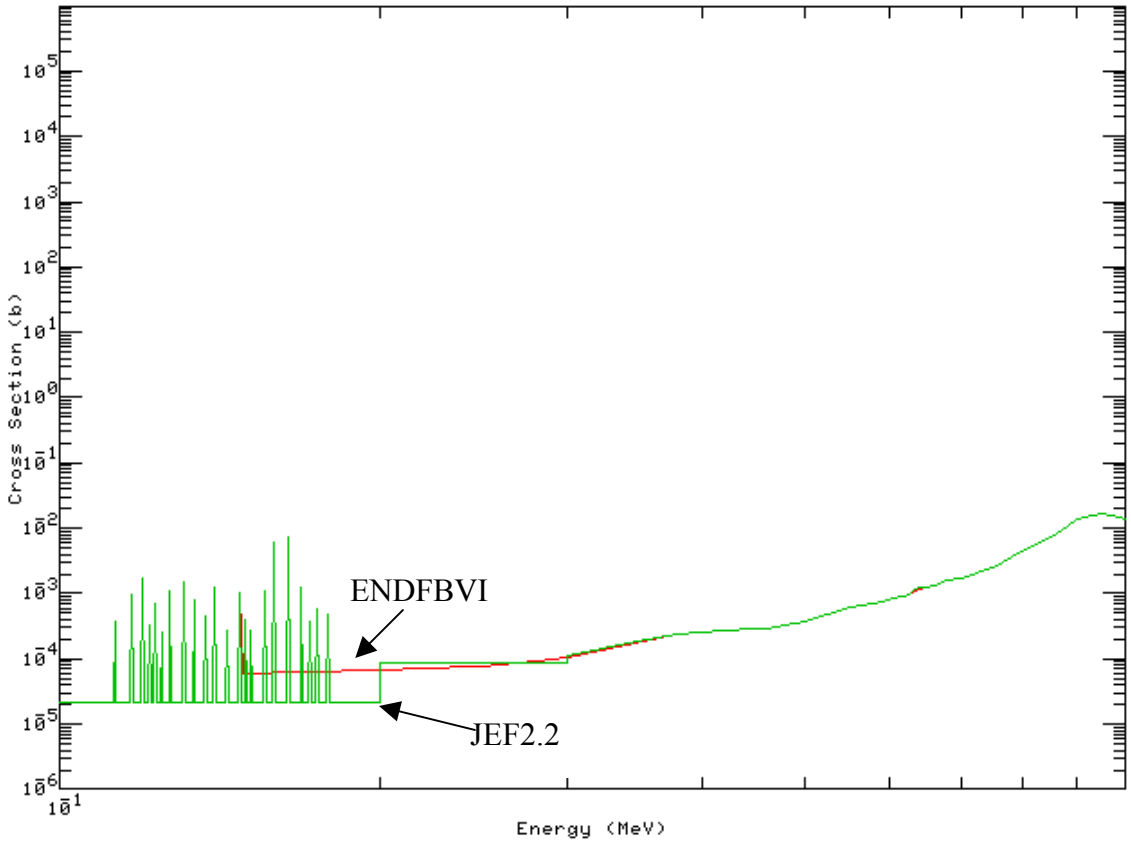


**Fig. A.4 Comparison of 238U Fission Cross Section Libraries**

## Fuel Cycle Economics (Pin Core)

The demonstration B&B GFR utilizes U15N fuel in a triangular pitch pin assembly. The $U^{15}N$ fuel is required from a neutronics standpoint for the pin-type assembly because of its low parasitic absorption and very high heavy metal density. While advanced fuel assembly designs such as the Tube-in-Duct will allow for higher loading with fuel such as UC, the more conventional assembly type demands a high performance fuel form to operate on the B&B fuel cycle.

The fuel cycle costs are therefore greatly compromised because of the costs of the highly enriched nitrogen (HEN). While U15N fuel is being investigated for several advanced fuel cycles, there is much debate over the cost of HEN. Cost estimates range between 10 USD/gHEN to 1,000 USD/gHEN.[1,2]

While extensive parametric analyses were done, a "reasonable" point case is shown below to determine what the cost of HEN must be for the demonstration plant fuel cycle cost to be competitive with an LWR. The three options investigated were: no reprocessing or recycle of any kind, reprocessing of the B&B GFR spent fuel and reuse in a PWR, and reprocessing of the B&B GFR spent fuel and reuse in the GFR as well as HEN recovery. As one can see from Figure A.5, the price of HEN must be on the order of 40$/gHEN for the demonstration B&B

GFR to have a comparable fuel cycle cost to a conventional PWR. The primary reason is that the fuel residency time is very large (18 EFPY) and hence a much larger fraction of the fuel cycle cost is the carrying charge, making the economic viability of the B&B GFR highly sensitive to the discount rate. It is evident that HEN costs must be in the range of 20 – 40 USD/g to permit competitive fuel cycle economics.

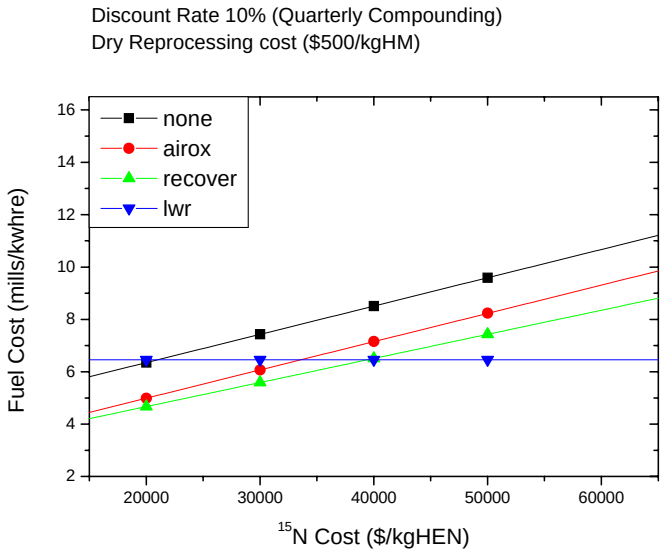


**Fig. A.5 Fuel Cycle Cost as a Function of HEN Cost**

## Fission Product Buildup and Spent Fuel Reprocessing (Pin Core)

AIROX-like reprocessing of spent B&B GFR fuel for disposition in a PWR has been investigated. The outcome of that analysis showed that Sm149 was the leading contributor to parasitic absorption in the treated fuel once loaded in a PWR (accounting for 1/3 of all parasitic absorption).[3] In a fast reactor spectrum on the other hand, MCNP was also used to calculate which of the over 60 tracked fission product nuclides had the largest absorption cross section, which was found to be $^{101}$Ru.

Since there are particular applications where some B&B GFR spent fuel may be recycled and used as PWR fuel, the buildup of these fission products was investigated. Figure A.6 illustrates that these fission products show no signs of approaching saturation after 150 MWD/kgHM of burnup. Therefore, while limited recycle into LWRs (by using hybrid assemblies, i.e. half fresh and half recycled fuel pins) using AIROX is possible at this burnup, it is unlikely that fuel with a larger discharge burnup may be useful as a PWR fuel unless improved processing which removes rare earth metals can be developed. In a GFR however, $^{101}$Ru is tolerable for several re-insertions.

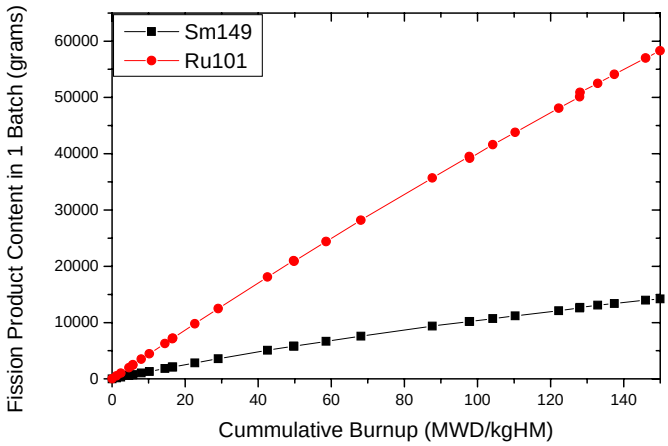


**Fig. A.6 Buildup of Dominant Fission Products in B&B Fuel**

## Core Physics INEEL

**Contributors: Kevan D. Weaver, J. Parry, Theron Marshall, Cliff Davis**

### Core Physics

The 1/8$^{th}$ MCNP core model was completed, and a reflector was added using the intermetallic $Zr_3Si_2$. Results of the reactivity limited burnup calculations were planned for this quarter, but problems with the parallel computing system were encountered. Calculations will resume once the problems are identified and corrected.

### Future Work

Burnup calculations will continue, and titanium will be used in the reflector.

**B&B GFR Fuel Cycle**

**Contributors: M. Driscoll, P. Yarsky (MIT)**

**Fuel Cycle Cost**

Fuel cycle costs of the B&B concept in the no-reuse mode are fairly straightforward. The steady-state reload fuel has the same enrichment as today's highest rated PWRs, namely 5 w/o U-235. The startup core batches have an average U-235 enrichment of 10 w/o. These two fuel types are readily costed out, as shown in Table A.2.

At the other extreme, fuel which is re-used has two major cost centers of uncertain magnitude: a chemical oxidation-reduction step without separation or removal of fission products (except volatiles) or actinides, followed by refabrication. Chemical processing is similar to the AIROX/DUPIC/OREOX treatment under evaluation in Korea and Canada for re-use of PWR spent fuel in CANDU reactors. Costs are claimed to be considerably less than for full-scale reprocessing. In Table A.1 the estimate is taken to be half the OECD/NEA estimate for conventional reprocessing of breeder reactor spent fuel; in contrast the refabrication cost is taken to be 1.5 times that of a fast reactor's TRU MOX reload because of the much higher radioactivity of B&B unpartitioned fuel.

**Table A.2 Direct [1] Front End Costs of B&B Fueling Options[2]**

| | Fuel Type | | |
|---|---|---|---|
| | Steady State<br>5 w/o U-235 | First Core<br>10 w/o U-235 | Re-used in GFR |
| Ore | 320 | 650 | -- |
| Enrichment [3] | 680 | 1600 | -- |
| Fabrication | 250 | 250 | -- |
| Redox Processing | -- | | 1000 [4] |
| Re-fabrication | -- | | 3900[5] |
| TOTAL ($/kg | 1250 | 2500 | 4900 |
| Burnup (MWd/kg) | 150 | 25-150 (6-batch fueling) | 150 (per re-insertion) |
| Mills/kwhre [7] | 0.87* | 10.4-1.74<br>Avg. = 6.1 | 3.4 |
| *compare to | 2.71 | for PWR Fuel at 60 MWd/kg, 32% efficiency (again without financial carrying charges) | |

Notes: (1) i.e., without carrying charges; costs are per kg HM in fuel
(2) Based on OECD/NEA reference cost values (0-1)
(3) Includes conversion
(4) AIROX type assumed half of conventional FBR reprocessing
(5) Assumed 1.5 times conventional FBR TRU MOX value
(6) Back end disposal costs not accounted for
(7) Assume thermal efficiency of 40%

As can be seen, the re-used fuel mills/kwhre cost is about twice that of fully burned startup fuel. In view of the extremely large uncertainty in the estimate, the costs may be considered roughly comparable to that of PWR fueling. Also note that first core fuel will be quite expensive for fuel removed before full burnup; hence their re-use will be particularly attractive.

For re-use in a PWR the same costs would apply except that blending with inexpensive natural uranium would take place to roughly double the amount of fuel mass in the reloads; on the other hand, burnup would be reduced to about 60 MWd/kg. Net mill/kwhre costs will exceed that of conventional fresh uranium fueling.

Based upon these first-order crude estimates, it is clear that the focus must be on improving and reducing processing and refabrication costs of GFR spent fuel. The most optimistic lower limit would be to use DUPIC cost estimates of 510 S/kg for processing plus refabrication of PWR spent fuel. Thus achievement of economic parity is not out of the question.

In the interim it may be worthwhile to investigate reinsertion of underburned first-core fuel as a booster for later steady-state reloads. One could also contemplate raising the steady-state reload enrichment from 5 w/o to 6 or 7 w/o. Since first core fuel has 10 w/o enrichment the cost of relicensing front end facilities to exceed the current regulatory limit of 5 w/o will have already been expended. There has also been some discussion of doing this for conventional PWR fueling.

**Cost of N-15**

Many GEN IV fast reactor designers are considering the use of enriched N-15 for their UN fuel. This appears to be an expensive proposition since natural nitrogen contains only 0.368% of this isotope. We have not been able to find definite cost projections. The following approximate analysis attempts to establish a rough range of potential costs.

The following approximate relation gives the separative work per unit mass of enriched product for a rare isotope enriched to a high concentration:

$$\frac{S}{P} \approx \left[ \frac{\ln\left(X_F / X_W\right)}{\left(X_F - X_W\right)} \right] \bullet X_P \qquad (1)$$

where $X_P$, $X_F$, $X_W$ = enrichment of product, feed and tails, respectively.

When applied to natural uranium enriched to 90 w/o, Eq. (1) predicts SWU within about 2% for 0.1 to 0.3 w/o tails. For nitrogen enriched to 95%, predicted SWU ≈ 440 kg/kg product for 0.1% tails assay. If SWU costs for uranium of about 100 $/kg are applied, then since 0.063 kg of N-15 are required per kg U, the cost of using N-15 is about 2800 $/kg HM. This should be compared to 5 w/o U-235 UN fuel using natural nitrogen at about 2000 $/kg.

For another estimate, one can note that the SWU required to enrich boron to 95% B-10 at 1% tails is about a factor of 30 less than the above N-15 requirement. For a B-10 cost of 10$/g one would then expect 300 $/g for N-15, with a resulting add-on to fuel cost of about $19,000.

It is clear, therefore why recovery and re-use of N-15 from spent fuel is essential from an economic point of view. This contravenes a major goal of the B&B concept if once-through operation is required.

**Tasks A.4 and A.5**

**Contributor: M. Driscoll (MIT)**

**Fuel Processing and Reuse**

The following findings summarize the current status of the Breed-and-Burn concept's ex-core fuel cycle:

1. One can make the B&B GFR work with UN-15 burned to 150 MWd/kg using steady-state reload fuel enriched to 5 w/o U-235 on a once-through basis.
2. GFR spent fuel, as $UO_2$ can be used in a PWR by blending with fresh U to reduce the Sm-149 concentration to the point where it functions as a useful burnable poison.
3. Fuel can be reconstituted and reinserted into the GFR as UN-15, and burned to 300 and perhaps 450 MWd/kg without fission product (FP) removal. Sm-149 builds up linearly vs. burnup as does Ru-101, the strongest FP absorber in the GFR spectrum.
4. Thus Sm-149 (and other RE/Lanthanide) removal would be very helpful for PWR re-use but not really needed for GFR re-use.
5. N-15 will be expensive. Based on SWU needed vs. B-10 and 10 $/g for the latter, N-15 will cost ≈ 300 $/g or about 18,000 $/kg HM for UN, compared to ≈ 2000 $/kg for 5 w/o fresh $UO_2$ or UC fuel. Hence recovery and re-use would be essential.
6. Thus we prefer to use UC fuel, in which case single-pass re-use in the GFR is probably necessary to make B&B work. Again, FP removal is not really necessary. But after discharge at 300 MWd/kg there is definitely too much Sm-149 for use in a PWR, in which case observation No. 4 applies even more strongly.
7. Hence processes are needed to make (fresh) and re-make (radioactive) VIPAC UN and UC for the GFR, and with significant RE removal if re-use as $UO_2$ in PWRs is to be practical.

**Kinetic Evaluation of Fission Element Removal by CARDIO**

**Contributors: Dustin Crawford, Thomas Hartmann, Ken Czerwinski (UNLV)**

Within this quarter work was performed on evaluating Sm removal and analysis of nitride fuels. Ongoing experiments were performed on mixed fission elements systems. ICP-MS experiments are being performed to evaluate removal kinetics for the mixed system. The addition of fission elements to uranium dioxide will be performed in the next quarter, with the synthesis of uranium dioxide performed in this quarter. The $UO_2$ is synthesized from the precipitation of uranyl nitrate with ammonia hydroxide. The precipitate is washed three times with water, heat to dryness at 80ºC, then calcined at 600ºC under air. The uranyl oxide solid is converted to $UO_2$ by heating under 4% $H_2$/96% Ar at 800ºC. The synthesized $UO_2$ was characterized by XRD. This $UO_2$ material will be used for experiments in the next quarter.

From our previous studies, removal yield of Sm at 1000ºC was found to be 0.69. The kinetic rate was found to be $0.77 \pm 0.09$ $min^{-1}$. The removal yield as a function of time for Sm at 1000ºC is shown in Figure A.7 below.

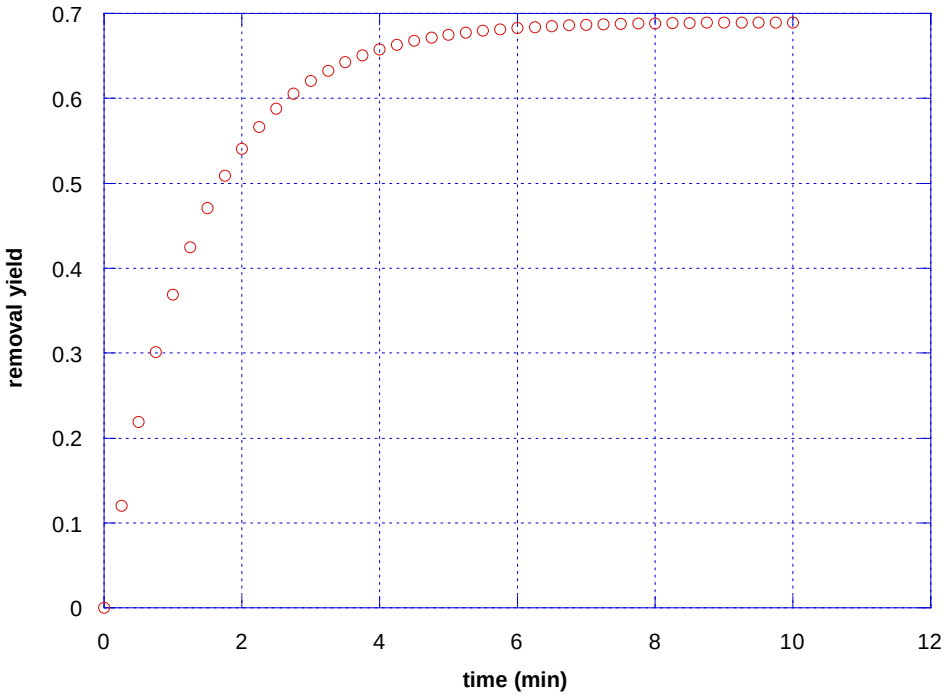


**Fig. A.7 Sm Removal vs. Time**

This data will be verified with further experiments.

Investigations into nitride fuels were performed this quarter. For the breed and burn project, UC can be used as the basis of UN synthesis using enriched $^{15}N$. Oxide ceramics are generally the starting point for UN as well as UC synthesis. Oxides are fabricated using a precipitation method. The process consists of dissolving and mixing the chloride or nitrate salts

in purified water, creating a precipitate with $NH_4OH$ or oxalic acid. The precipitate is washed with acetone and purified water, milled, and dried at 90ºC. The dried precipitate is milled again and redried at 150ºC for 2-3 hours. It is milled again and then calcined at 750ºC for 1 hour. The calcined powder is milled and then cold pressed into 13 or 7 mm diameter pellets for 2 minutes before being sintered under a mixture of argon and 4% hydrogen for four hours at 1500ºC. Nitride ceramics are produced using the carbothermic reduction process (Ref 1). In this process carbon is added in excess to actinide oxides. Under Ar conditions carbides can be formed. If the mixtures are heated in the range of 1500°C under a stream of $N_2$ gas then carbon dioxide is liberated and the actinides converted to the nitride. The carbon dioxide concentration in the outgas is used to monitor the reaction. The gas is change to a reducing mixture upon the reduction of $CO_2$ in the gas phase. The outgas monitoring can also be used to assess the nitrogen stream in the CARDIO process, expected to be nitrogen oxides under the $CO_2$ atmosphere. The recovery of enriched nitrogen from UN has been investigated elsewhere (Ref 2). In this work the dissolution of spent nitride fuel with an oxidizing agent in molten salt was examined. Most of nitrogen is recovered as $N_2$ gas resulting from the reaction of uranium nitrides above 550ºC. The formation of intermediate compounds was seen below with temperature. This system can be used as the basis for the recovery of $^{15}N$ from nitride fuels in the CARDIO process. However, the speciation of nitrogen under $CO_2$ at elevated temperatures will need to be evaluated to fully determine if the recovery process is feasible.

Our work on ZrN and CeN ceramics from other projects has shown the presence of oxides in the nitrides from the carbothermic reduction (see microprobe--Figure A.8). This seems to stem from the furnace material, an oxide rather than a metal. This observation is correlated with laser flash diffusivity measurement recently performed on nitrides for the Advanced Fuel Cycle Initiative program, showing the formation of oxides from nitride due to furnace materials. This oxide formation is also evident with UN fuels, where surface coating by $UO_2$ occurs.

**References**


1. W.O. Greenhlagh, "Kinetic Measurements for the Carbothermic Synthesis of Uranium Nitride, Plutonium Nitride, and (Uranium, Plutonium) Nitride. J. Amer. Cer. Soc. **56(11)**, 553-7 (1973).
2. H. Hayashi, F. Kobayashi, T. Ogawa, K. Minato, **"**Dissolution of Uranium Nitrides in LiCl-KCl Eutectic Melt", J. of Nucl. Sci. and Tech., (Suppl. 3), 624-627, (2002).

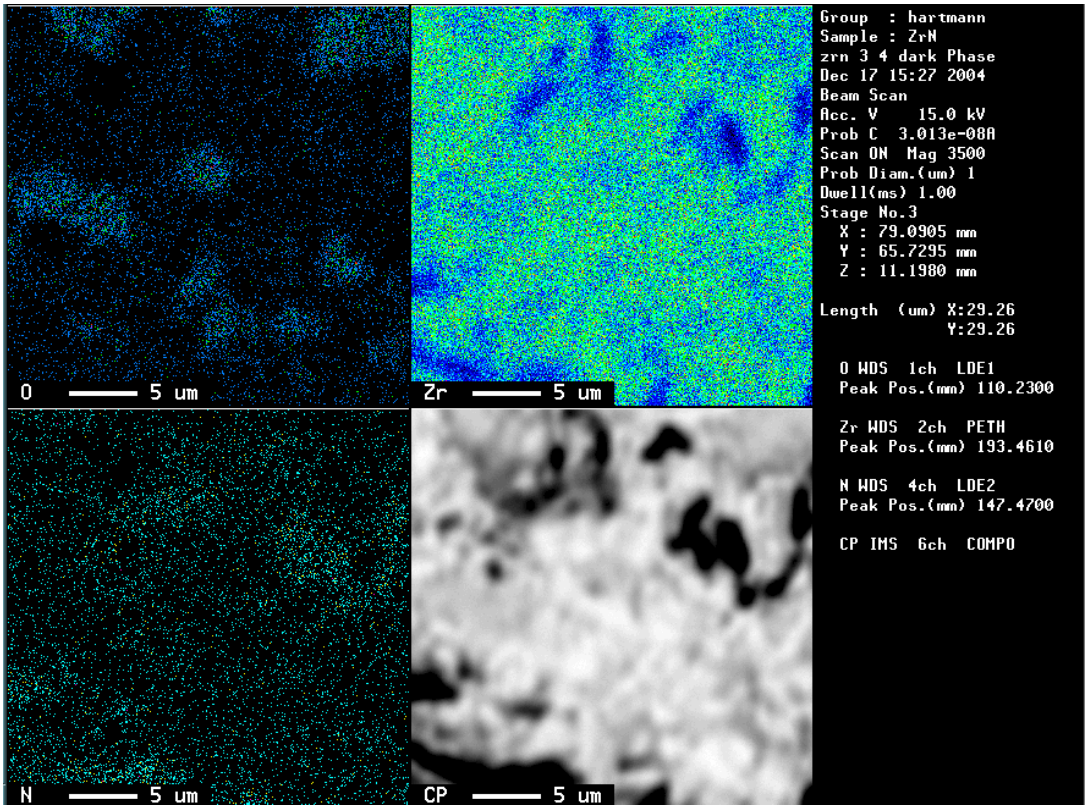


**Fig. A.8 Microprobe of ZrN and CeN Ceramics**

**Tasks B and C: Core Thermal Hydraulics and Plant Design**

**Task B/C.1 Thermal-Hydraulic Modeling at INEEL**

**Contributors: Kevan D. Weaver, James Parry, Theron Marshall, Cliff Davis**

Research at the INEEL continued to focus on systematically developing a representative RELAP5/ATHENA model of the helium-cooled option for the 600 $MW_t$ GFR. During this quarter, several improvements were made to the ATHENA model:

1) The ATHENA model initially considered the containment building (CB) to be a single volume, as shown in Figure 1, with the reactor vessel located just above floor level. The model was improved by adding a reactor cavity compartment (RCC). The reactor vessel was placed inside of the RCC and the RCC exists inside of the CB (refer to Figure 2). The side walls and ceiling of the RCC are lined with the conduction panels of the Reactor Cavity Cooling System, which removes the radiative and convective heat from the reactor vessel. The RCC floor has a stainless steel liner in order to protect the concrete floor from thermal decomposition.

2) During normal operations, the RCC is isolated from the CB. However, when the RCC is pressurized by He from the LOCA, a burst valve opens and gas exchange is permitted between the RCC and the CB. Subsequent ATHENA analysis did not demonstrate significant air-He exchanges between the RCC and the CB during the LOCA. The CB was then re-modeled as a four compartment building, as shown in Figure 3. The flow areas of the junctions that connect each CB volume were appropriately sized so that there were no flow restrictions. The junctions were also given no form losses. While the CB is modeled as four connected volumes, the total volume for the CB was maintained. Essentially there was still one large CB, but the four volumes allowed an air circulation path to exist. The ATHENA analysis showed that a parasitic radiative heat from the RCC induced a fair amount of air circulation within the CB during normal reactor operations and the expected air-He exchange during the LOCA.

3) The ATHENA model was revised to use the Gnielinski correlation. The previous INEEL GFR-He LOCA calculations used the Dittus-Boelter correlation to calculate heat transfer rates to the He. However, research and calculations by INEEL staff strongly suggested that future GFR-He analyses use the Gnielinski correlation because its predictions were more consistent with existing data from heat transfer experiments. The ATHENA GFR-He model was analyzed using the Gnielinski correlation and the steady-state peak fuel temperature was approximately 100 ºC higher than the one that ATHENA predicted when using the Dittus-Boelter correlation. The fuel temperatures during the LOCA transient using the Gnielinski correlation have not been calculated due to work that was performed on the $CO_2$ injection system.

4) Prior to revising the ATHENA model to use the Gnielinski correlation, a large tank of $CO_2$ was added to the ATHENA model. A pipe from the $CO_2$ tank to the inlet plenum of the reactor was included. Figure 4 presents a schematic of the ATHENA $CO_2$ injection model. There is a check valve in the pipe that prevents $CO_2$ flow to the reactor when the reactor's pressure is above 1.6 MPa. The check valve's actuating pressure was arbitrarily selected for this initial analysis with the understanding that the actuating pressure will later be selected based upon sensitivity studies. Unfortunately, the ATHENA analysis failed once the LOCA was initiated and $CO_2$ was injected into the inlet plenum. The analysis failed as a result of ATHENA predicting the occurrence of liquid He, which is physically impossible given the temperature and pressure at the time of the code's failure. Staff at the INEEL have been working to resolve the ATHENA problem. Until the time of this analysis, ATHENA users did not have models that required the He properties to be below the critical temperature. ATHENA was previously updated to resolve this situation when water was used, but not for He. Other users have confirmed that the same system error occurs when they attempt to inject either $N_2$ or $CO_2$ as a non-condensable with He.

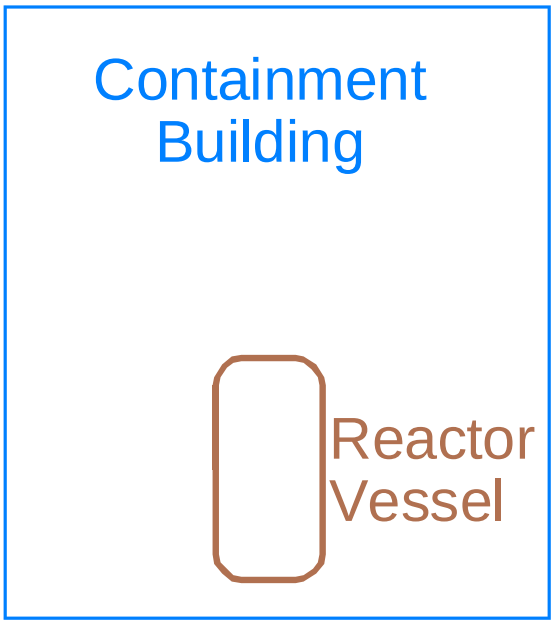


**Fig. B/C.1 Initial ATHENA Model of the Containment Building**

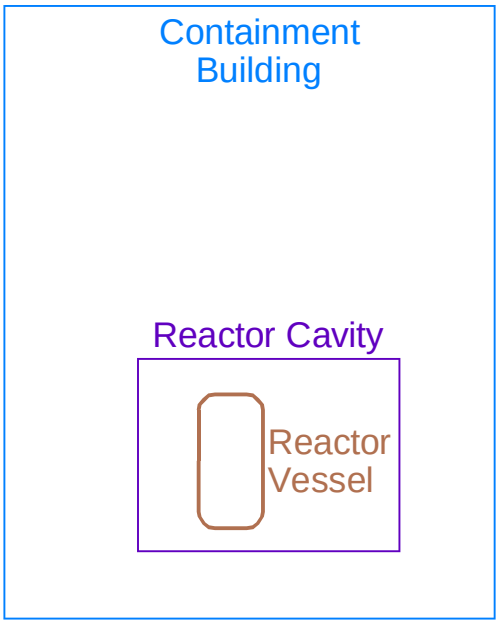


**Fig. B/C.2 ATHENA Model of Containment Building and RCC**

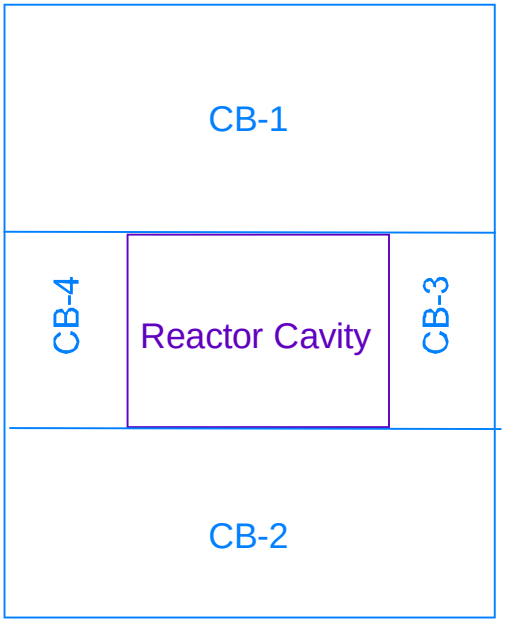


**Fig. B/C.3 Four Volume Configuration for the Containment Building**

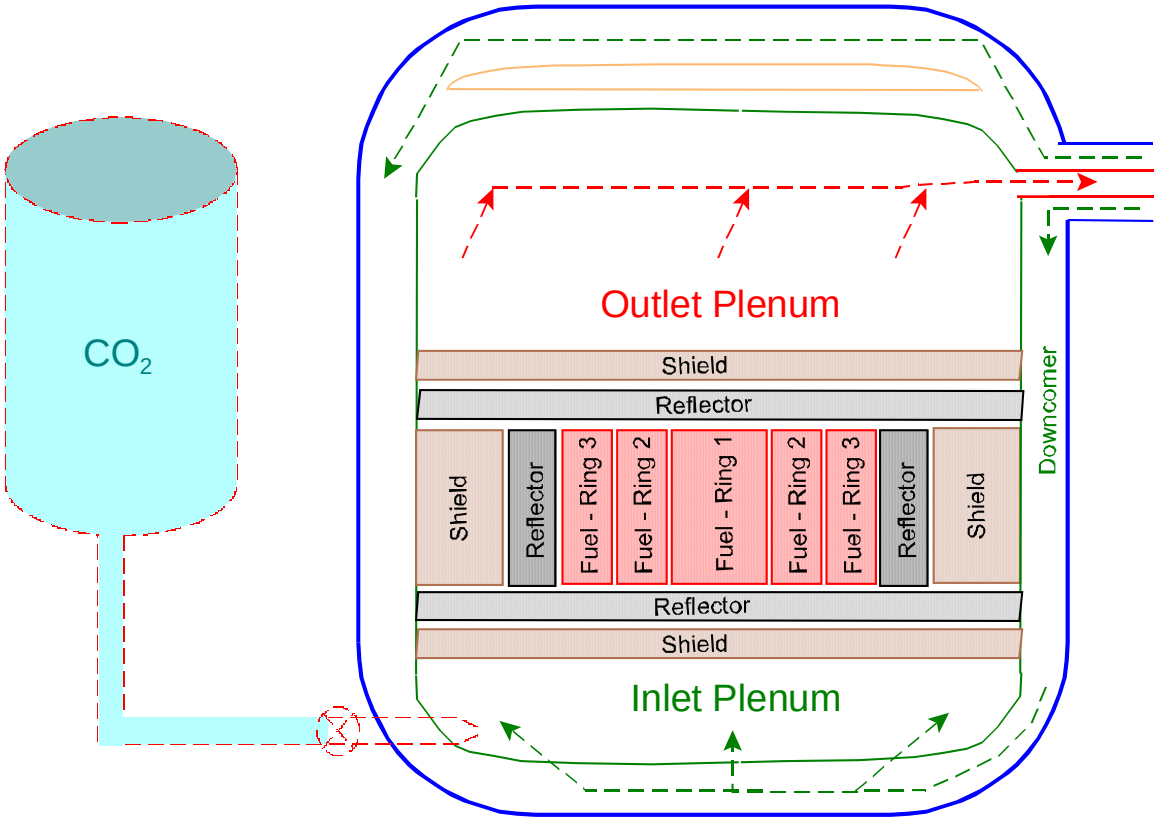


**Fig. B/C.4 Schematic of ATHENA Model for GFR-He Design with $CO_2$ Injection System for LOCA**

**Task C Plant Design**

**Shutdown Heat Removal**

**Contributor: M.J. Driscoll (MIT)**

The recent decision to change to a Rankine cycle power conversion system also increases the diversity and redundancy of decay heat removal modes. As in the final version of the GA GCFR design of the 1970's we now have

1. Auxiliary cooling loops (3 @ 50% each), as previously designed for our S-$CO_2$ PCS version of the GFR
2. A similar parallel system using the main steam generators as heat sinks and a pony motor on the main circulator shaft.

The first of these systems is designated the CACS (core auxiliary cooling system) and the second as the SCSC (shutdown cooling system) by GA. As with recent MIT designs, including those from our INERI under ANL/CEA leadership, their CACS has both active and passive mode capabilities.

Based upon analyses for CACS-only protection recently completed at MIT (2) and earlier analyses for the GA-GCFR (3), extremely low core damage frequencies are anticipated. As noted in Ref (2), the CDF contribution due to a LOCA is $7.58 \times 10^{-8}$ per reactor year for 3 loops @ 100% capability each. More loops confer very little additional benefit—hence the GA SCS may not in fact be all that useful.

The B&B core has another advantage should one wish to exploit it as a last resort option: flooding the core with water gives a negative reactivity contribution due to the low coolant volume fraction required for satisfactory B&B performance.

**References:**


1. GA-10298 Amendment 10, "GFR Residual Heat Removal System Criteria, Design and Performance", Sept. 1, 1980
2. M.J. Delaney, G.E. Apostolakis, M.J. Driscoll, "Risk-Informed Design Guidance for Future Reactor Systems", accepted for publication in Nuclear Engineering and Design.
3. P. De Laquil, "An Accident Probability Analysis and Design Evaluation of the Gas Cooled Fast Breeder Reactor Demonstration Plant", PhD Thesis, MIT Nucl. Eng. Dept., 1976

## Task D: Fuel Design

### D.1. Task Status and Significant Results

**Contributors: D. Wachs (ANLW)**

**Current Status**

The development of a model based on the benchmark parameters to predict the fuel thermal conditions was the focus of the last quarter. The results of the analysis will be compared to those returned by the system level analysis performed by researchers at the INEEL and MIT to confirm consistency.

The fuel configuration was assumed to consist of tubes in a vented duct with ODS cladding and VIPAC uranium carbide fuel. Model development is ongoing and results will be reported in the next quarterly. The selection of the duct size was made somewhat arbitrarily for this analysis and must be revisited in future work to determine the optimum size.

**Future Work**

Following the feasibility study stage of the proposed fuel design an assessment of the fabricability and expected performance of the fuel is required. Both areas will be addressed in the remaining year 3 efforts. In the area of fabrication, the assembly of ducts will be examined to evaluate duct forming and joining techniques and their likely impact on performance. These issues are non-trivial challenges associated with the baseline selection of ODS cladding materials. An estimation of the likely fuel performance will also be performed. Issues examined, for example, will include non-uniform densification of fuel (due to sintering at non-uniform temperatures), macroscopic dimensional change and its impact on structural integrity of cladding, and fission gas release/retention.

**Future Work**

The principal focus in the next two quarters by all participants will be on iterative adjustment and optimization of core thermal-hydraulics to meet cladding temperature constraints (peak and average) under steady-state, operational transient and severe accident conditions. A second set of constraints to be met involve the neutronics of UC fueled cores, which require the highest practical fuel volume fraction compatible with a tolerable pressure drop which will not lead to excessive circulator power consumption and the consequential loss of overall plant thermodynamic efficiency.

The thermal-hydraulic numerical benchmark in Appendix C will assure that the three research groups involved all start with a compatible reference case.

Looking ahead to meeting the 9/30/05 end-of-project commitments, we are in the process of developing two major topical report outlines: one on core design, to encompass both reactor physics and thermal-hydraulics; and the other on ex-core GFR system designs suitable for hosting a B&B core.

## Appendix A Indirect He-to-S-$CO_2$ Brayton vs. He-to-Rankine Cycle Comparison

System design studies carried out on our Breed & Burn GFR project have shown that the Rankine alternative is preferable because of the large primary circulator power associated with the S-$CO_2$ cycle.

Gezelius derives the following relation for circulator power (Ref 1)

$$\frac{W}{Q} = \frac{10^{-3}\,\mathrm{Pr}^{2/3}\;Q^2}{\left(\rho^2 C_p^3\right)\;A_f{}^2\;\;\Delta T_f\;\;\Delta T_c^2} \tag{1}$$

Where:

| | |
|---|---|
| $C_p$ | Heat capacity, kJ/kg °C |
| $\rho$ | Density, kg/m$^3$ |
| $W$ | Circulator power, kW |
| $Q$ | Channel thermal power, kW |
| $A_f$ | Transverse flow area, m$^2$ |
| $A_s$ | Heat transfer surface area, m$^2$ |
| $\Delta T_c$ | Coolant temperature rise in channel °C |
| $\Delta T_f$ | Channel average heat transfer film drop, °C |
| $Pr$ | Prandtl Number ≈ 0.7 |

In the present case thermal power, flow area pressure and temperature are fixed. Furthermore the Prandtl Number is a constant, in which case:

$$\frac{W}{Q} \approx \frac{1}{M^2\;\;C_p{}^3 \Delta T_f\;\;\;\Delta T_c^2} \tag{2}$$

Where $M$ = molecular weight of gas

One can also eliminate $\Delta T_f$ using the same relations as applied by Gezelius:

$$\Delta T_f \approx \frac{1}{k}\left(\frac{C_p\;\;\Delta T_c}{Q}\right)^{0.8} \tag{3}$$

To obtain:

$$\left(\frac{W}{Q}\right) \approx \left[\frac{k}{M^2\;\;C_p{}^{3.8}}\right]\left[\frac{1}{\Delta T_c^{2.8}}\right] \;\approx\; \frac{1}{\Delta T_c^{2.8}} \tag{4}$$

for the same coolant (He).

A primary system having a minimized core outlet temperature, coupled to an optimized S-$CO_2$ cycle will have a $\Delta T_C$ of about 150°C, while British SGR Ranking cycle units have a core $\Delta T$ as large as 385°C: a factor of 1.75 greater. This reduces (W/Q) by a factor of $(2.75)^{2.8} = 17$ according to Eq. (4).

One is therefore motivated to investigate increasing $\Delta T_C$ to reduce mass flow rate since circulator power is proportional to mass flow rate cubed.

Figure AA.1 shows the range of possible temperatures across the IHX, $\Delta T_C$, in an indirect Brayton cycle. Points to note are:

1. $\Delta T1$ and $\Delta T2$ must be positive to sustain heat transfer.
2. $T_{RO}$ is constrained to narrow range (at ≈400°C for a $T_{TI}$ of 550°C) by power cycle requirements to achieve high efficiency; this also applies to $\Delta T_{PC}$
3. The balanced profile requires the highest primary side mass flow rate, but minimizes the core outlet temperature
4. The skewed profile reduces primary side mass flow rate (hence pressure drop and circulator power) at the expense of a higher core outlet temperature. The higher log mean $\Delta T$ across the IHX also reduces the size of that component.

Since our metal clad fuel GFR core is strongly constrained by allowable maximum clad temperature, which in turn is determined by coolant exit temperature, the use of a skewed temperature profile is not a panacea. Furthermore, since core pressure drop dominates, reducing IHX size is only marginally beneficial. A circulator power penalty of at least a factor of five appears inevitable.

Hence we conclude that the Rankine cycle is preferable for B&B applications. (This may not be the case for other applications in which the option space for changing core design is larger). Adopting the Rankine cycle also greatly reduces the up-front R&D required before a B&B system could be deployed.

Reference

(1) K. Gezelius, M.J. Driscoll, P. Hejzlar, "Design of Compact Intermediate Heat Exchangers for Gas Cooled Fast Reactors", MIT-ANP-TR-103, May 2004

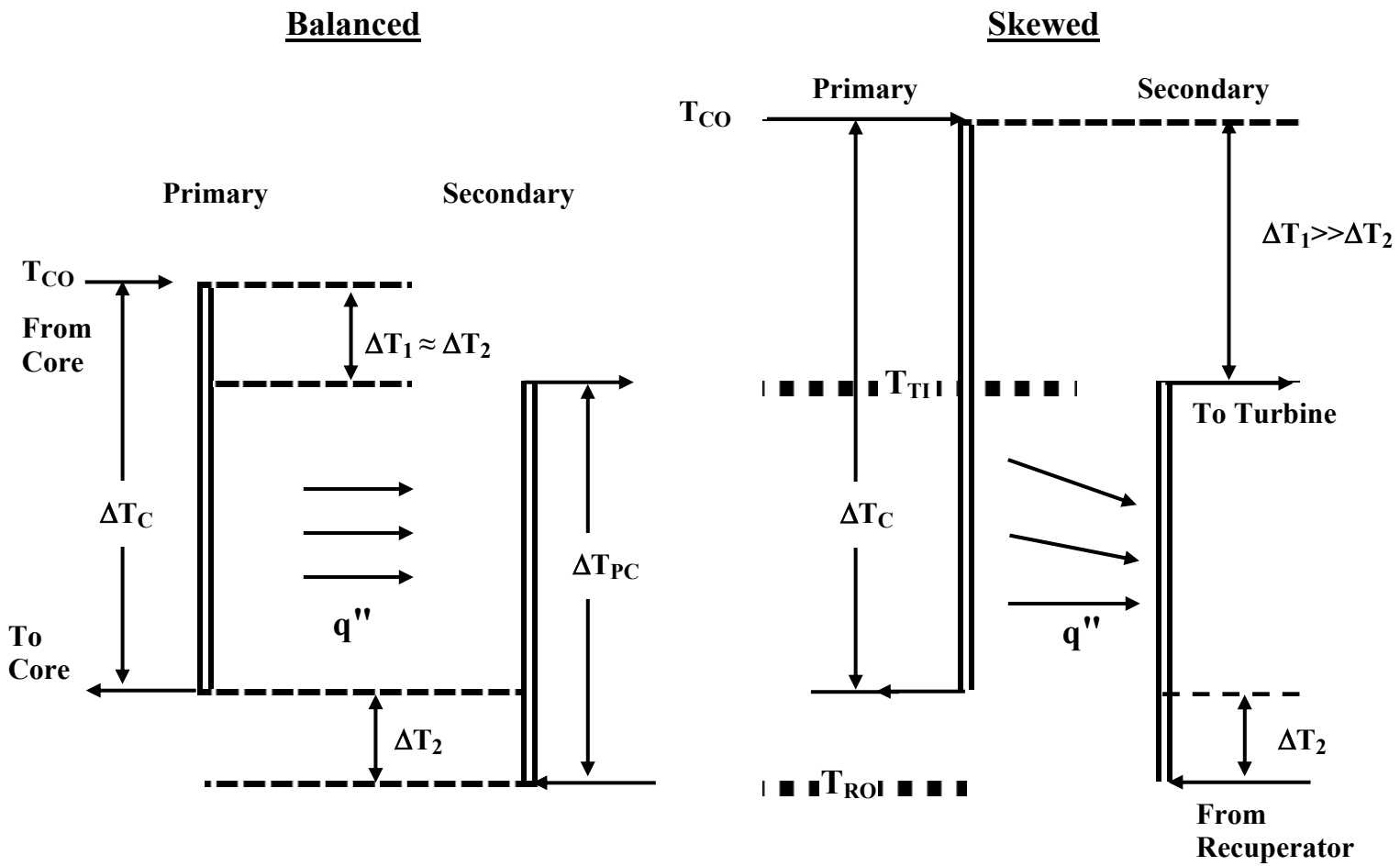


Key

| | | |
|---|---|---|
| | $T_{CO}$ | = Core Coolant Outlet Temperature |
| | $T_{RO}$ | = Recuperator Outlet Temperature |
| | $T_{TI}$ | = Turbine Inlet Temperature |
| | $\Delta T_1$, $\Delta T_2$ | = IHX Temperature Differences |
| | $\Delta T_{PC}$ | = Power Conversion System $\Delta T$ Which Determines Log Mean Temperature Difference |

**Fig. A-A.1 Intermediate Heat Exchanger (IHX) Temperature Profiles**

**Appendix B: An Advanced Vented Fuel Assembly Design for GFR Applications**

M.A. Pope, P. Yarsky, M.J. Driscoll, P. Hejzlar, P. Saha

*Nuclear Science and Engineering Department, Massachusetts Institute of Technology*
*77 Massachusetts Ave., 24-215, Cambridge, MA, 02139*
*mapope@mit.edu, yarsky@mit.edu, mickeyd@mit.edu, hejzlar@mit.edu, psaha@mit.edu*

## INTRODUCTION

For GEN-IV applications, fast gas-cooled reactor fuel must operate at high power density (hence high heat flux) and preferably at high volume fraction fuel and under large differential pressure-induced stresses, with heat transfer inferior to liquid-cooled alternatives. The design described here has evolved over the past several years as part of NERI and INEEL supported work at MIT to meet the constraints these circumstances impose: in particular that on allowable peak clad temperature.

## DISCUSSION AND DESCRIPTION

Figure 1 shows the basic concept: a tube-in-duct (TID) arrangement with coolant inside cladding tubes surrounded by vibrationally-compacted (VIPAC) fuel. The assembly is vented, as in the GCFR designs of the 1970's, to virtually eliminate pressure-induced stresses. However our focus here is not on this mechanical/materials feature, but on the thermal-hydraulic advantages conferred by the advanced coolant tube design shown in Figure 2: a "telescope" configuration with a larger diameter tube uppermost (i.e. downstream). This section also contains a helical wire or twisted tape to augment heat transfer.

This arrangement confers the following benefits:

1. The increase in upper tube diameter:
   a. Decreases the smooth tube pressure drop considerably more than it does the heat transfer coefficient, thereby enabling a further $\Delta P$ vs. Nu tradeoff using helical wire or twisted tape (1) to considerably augment heat transfer without a large net increase in pressure drop. Overall a factor of two reduction in gas heat transfer film $\Delta T$ appears practicable.
   b. Reduces fuel volume fraction in the upper region of the core. This further reduces local power, hence heat flux, and thus gas film temperature drop. Heat transfer area is also increased. Reducing fuel volume fraction at constant enrichment is preferable to zoning enrichment for very high burnup, since in a fast reactor the latter strategy leads to a large unfavorable shift in axial power toward a cosine shape as burnup (and breeding) proceeds. Reduced fuel and increased metal volumes, of course, penalize neutronic reactivity.
2. Compared to a conventional unvented pin-type core, the coolant-in-tube approach eliminates spacer and gas plenum pressure drops—which then become available in the clad temperature reduction tradeoff process.
3. By reducing the pressure drop, hence primary circulator power, needed to attain an acceptable clad temperature, indirect gas-to-gas power plant designs can be devised without excessive net thermodynamic efficiency losses.
4. In general, reduced pressure drop also enhances natural convection (at elevated pressure) in post-accident scenarios and refueling shutdowns. However, detailed evaluation of hot channel flow starvation under laminar flow conditions for helium coolant is necessary (2), especially in conjunction with heat transfer augmentation features.
5. If further power shape tailoring is required, one can dilute the (same enrichment) fuel in the upper region using increased void content or neutronically and chemically inert materials such as CeO, BeO or SiC: a universally useful tactic for fast reactors.
6. Compared to a pin geometry fuel element, the "inside-out" unit cell has roughly half the peak and average temperature rises from the clad surface to the peak interior value: e.g. see Ref (3). This reduces release of fission gases and other fission products, and fuel swelling, as well as stored energy at the outset of severe transients.
7. Because of the lower fuel temperature and reduced pressure drop compared to conventional pin-type cores, the alternative strategy of increasing core average fuel volume fraction (hence reducing coolant fraction) becomes possible. This will improve core neutronics (reduce enrichment, leakage and coolant void reactivity gain, increase conversion ratio), and hence fuel cycle economics.

## CONCLUSIONS

A high performance fuel assembly design for GFRs has been conceptualized which allows significant reduction of peak metal clad temperature, hence creep, without an excessive penalty in terms of core pressure drop and circulator power. In parallel with further thermal-hydraulic refinement, an evaluation is being carried out on the fission product gas venting/pressure equalization system. A high temperature version using SiC coolant tubes will also be evaluated.

## REFERENCES


1. F. KREITH, M.S. BOHN, *Principles of Heat Transfer*, 4th Edition, Harper and Row, p.628 (1986)
2. P. HEJZLAR, W.C. WILLIAMS, M.J. DRISCOLL, "Hot Channel Flow Starvation of Helium Cooled GFRs in Laminar Natural Convection", *Trans. Am. Nucl. Soc.*, **91**, (2004)
3. R. HANKEL, "Stress and Temperature Distributions", *Nucleonics*, **18**, No. 11 (Nov. 1960)

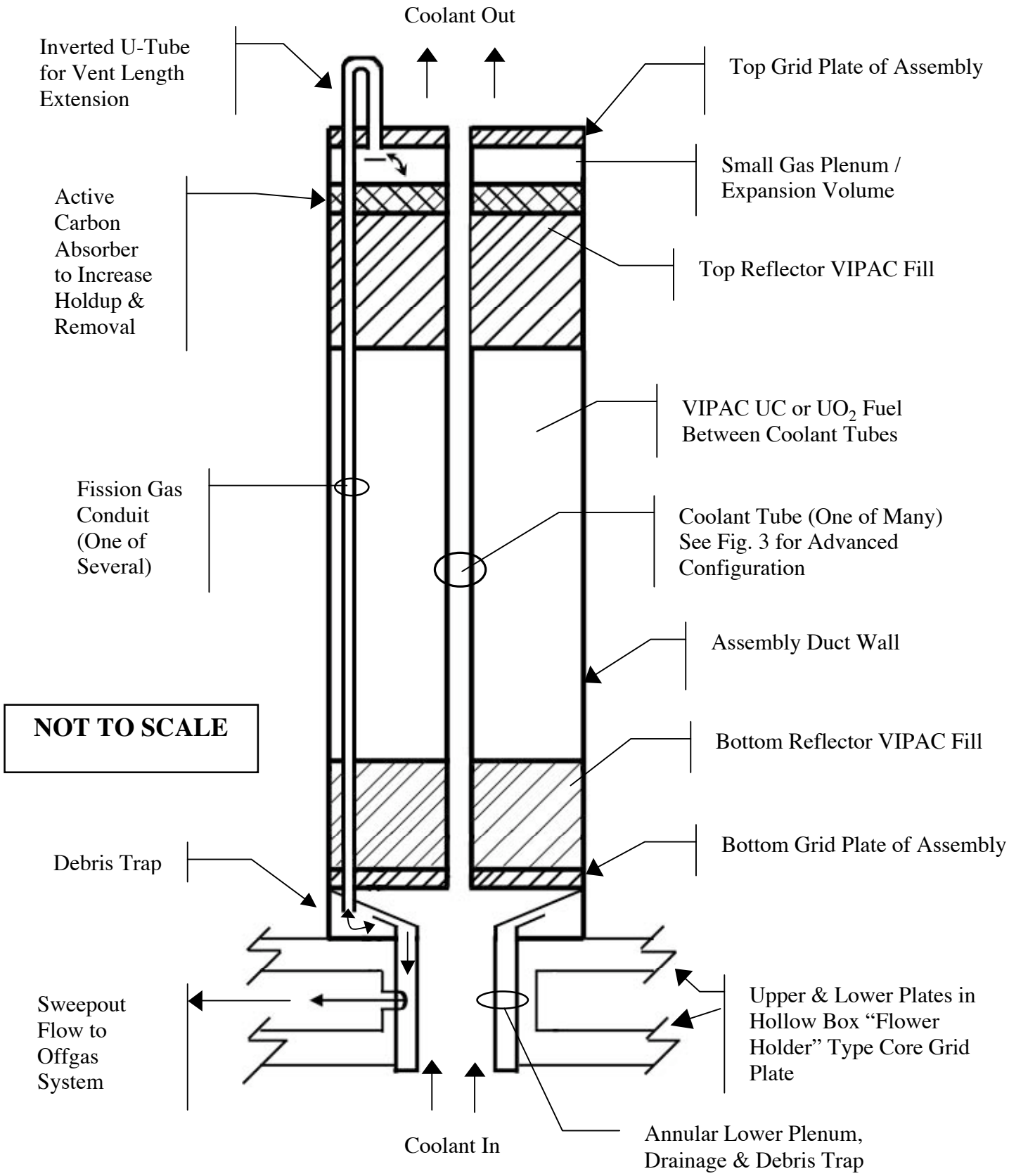


**Fig. A-B.1 TID Assembly Vertical Cross-Sectional View**

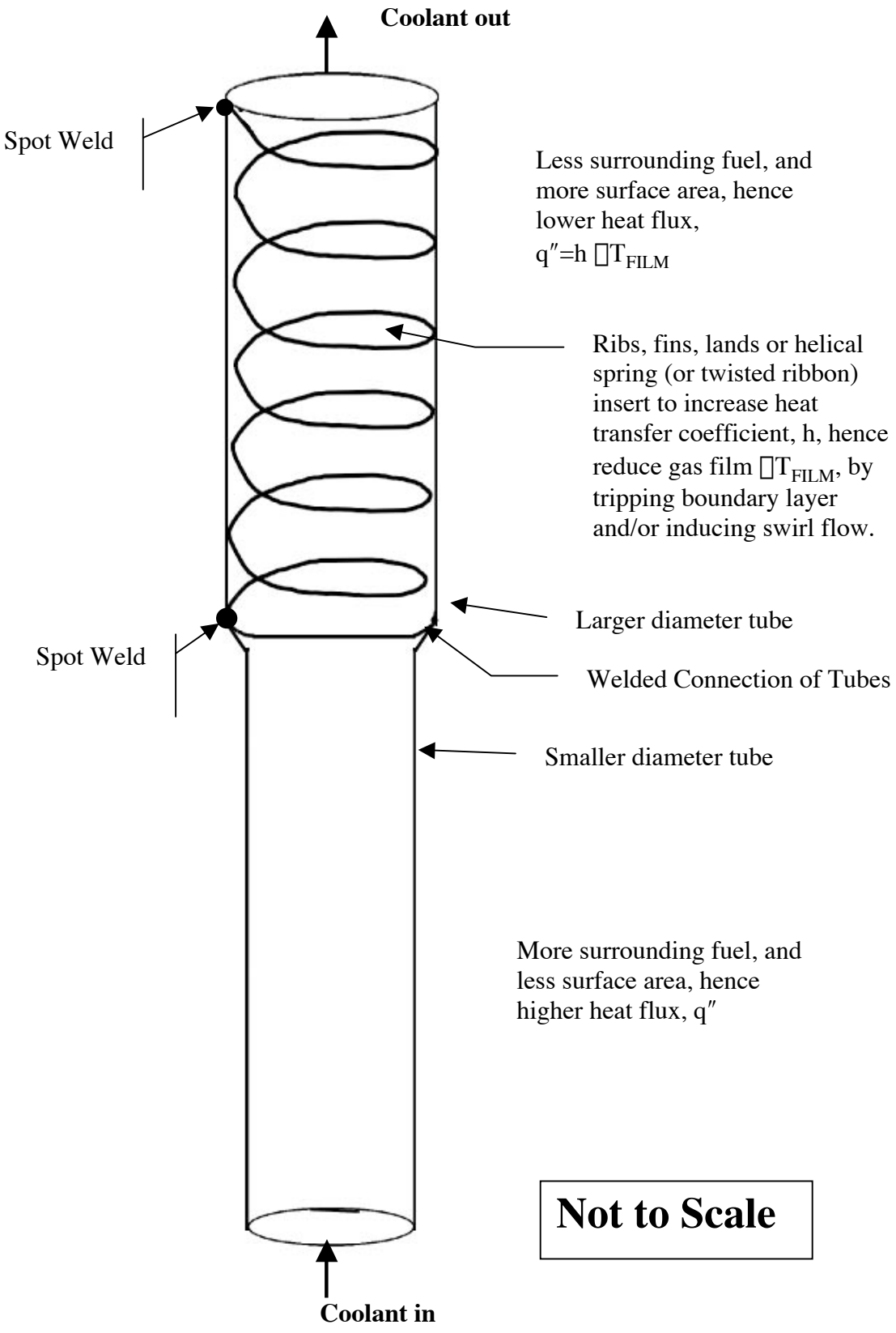


**Fig. A-B.2 Advanced TID Coolant Tube Configuration**

## Appendix C Numerical Benchmark Specifications for TID Fuel Assembly

**Contributor: M.A. Pope**

The tables and text which follow specify the parameters for a reference case Tube-In-Duct (TID) GFR core. See Appendix B for a more detailed description of this configuration.

The objective of this reference case numerical exercise is to provide the three laboratories involved in B&B core assessment–MIT, INEEL, and ANL-West–with a common starting point for their ensuing optimization and transient performance studies.

The results of an MIT in-house code run are also included. Temperatures for the average and hot channels (channel 1 and channel 2 respectively) are given at each axial node. *Twall* is the cladding surface temperature in contact with the coolant, *Tcmax* is the cladding surface temperature in contact with the fuel, and *Tfmax* is the fuel centerline temperature assuming an equivalent annulus of fuel rather than the actual triangular lattice.

In the average channel, the maximum clad hot spot temperature is 650.2°C and the maximum fuel temperature is 679.0°C. In the hot channel, the maximum clad hot spot temperature is 844.6°C and the maximum fuel temperature is 895.6°C. The cladding temperatures in the hot channel are excessive for our ODS cladding, even though it is pressure-stress free in a vented assembly. Thus future modifications are in order to reduce the clad hot sport to less than 750°C.

The fuel temperatures are far below likely limits. Note, however**,** that a rigorous conductivity model for VIPAC fuel has not been employed, nor has the reduction in fuel thermal conductivity due to irradiation been accounted for here. Nevertheless, even with more accurate fuel conductivity models, fuel temperature limits are not expected to be limiting, but rather clad temperature limits will drive much of the thermal-hydraulic design.

**Table A-C.1 Parameters for a Numerical Benchmark of T&H Models**

| | |
|---|---|
| Core Thermal Power | 2400 MW |
| Average power density | 128 kW/liter |
| Axial peaking factor, chopped cosine | 1.4 |
| Radial peaking factor | 1.77 |
| Number of channels | 59744 |
| Unit Cell Pitch | 1.3468 cm |
| Coolant Channel Diameter, $D_{c,i}$ | 1 cm |
| Cladding thickness, $t$ | 0.8 mm |
| Volume Fraction Coolant, $\upsilon_c$ | 0.500 |
| Volume Fraction Cladding, $\upsilon_{clad}$ | 0.1728 |
| Volume Fraction Fuel, $\upsilon_f$ | 0.3272 |
| Diameter of Equivalent Fuel Annulus, $D_{EA}$ | 1.414 cm |
| Channel height, $H_{chan}$ | 280 cm |
| Fueled height, $H_{core}$ | 200 cm |
| Helium Coolant inlet pressure, $P_{in}$ | 10 MPa |
| Helium Coolant inlet temp, $T_{in}$ | 420 °C |
| Helium Coolant mass flow rate | 3183 kg/s |
| Fuel form | UC VIPAC, 91% TD |
| Effective core diameter | 345 cm |
| Average Heat Flux | $6.39 \times 10^5$ W/m$^2$ |
| Max Heat Flux (average channel) | $8.96 \times 10^5$ W/m$^2$ |
| Max Heat Flux (hot channel) | $1.59 \times 10^6$ W/m$^2$ |

Following are notes on methodology for production of benchmarking results.

Use the Gnielinski friction factor formula good for smooth channels and Re>2300. [1]

$$\frac{1}{\sqrt{f}} = 1.8\log(\mathrm{Re}) - 1.5$$

The corresponding Nusselt number good for both uniform wall heat flux and constant $T_{wall}$ is given by

$$Nu_{FT} = \frac{\left(\frac{f}{8}\right)(\mathrm{Re}-1000)\mathrm{Pr}}{1+12.7\sqrt{\frac{f}{8}}\left(\mathrm{Pr}^{2/3}-1\right)}$$

[1] Gnielinski, V., "New Equations for Heat and Mass Transfer in Turbulent Pipe and Channel Flow," International Chemical Engineering, Vol. 16, No. 2, pp. 359-368, 1976. Note that this is a Darcy friction factor.

Channel entrance and exit losses are given by

$$\Delta P = K\frac{\rho v^2}{2} \quad , \quad K_{in} = 0.5 \; , \quad K_{out} = 1.0$$

A horizontal cross-section of unit cell is shown below.

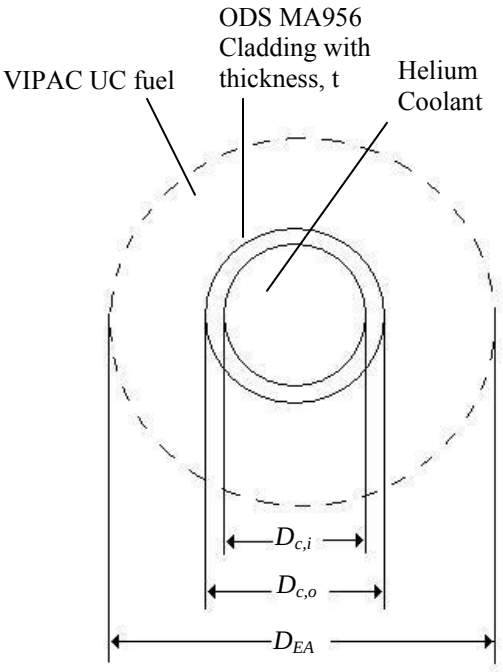


$$t = \frac{1}{2}\left(D_{c,o} - D_{c,i}\right)$$

**Fig. A-C.1 Horizontal Cross-Section of Unit Cell**

The actual unit cell is hexagonal with flat-to-flat width = 1.347 cm

One can relate these diameters to volume fractions in the following way. First, the volume fraction occupied by cladding is given by

$$\upsilon_{clad} = \upsilon_c\left[\left(\frac{D_{c,o}}{D_{c,i}}\right)^2 - 1\right]$$

Where,
$\upsilon_c$ = volume fraction occupied by coolant
$\upsilon_{clad}$ = volume fraction occupied by cladding
$D_{c,i}$ = inner cladding diameter in cm
$D_{c,o}$ = outer cladding diameter in cm

Then the fuel volume fraction is given by

$$\upsilon_f = 1 - \upsilon_c - \upsilon_{clad}$$

Where,

$\upsilon_f$ = volume fraction occupied by fuel

And finally, the diameter of the "equivalent annulus" of fuel in each unit cell is given by

$$D_{EA} = \frac{D_{c,o}}{\sqrt{1-\upsilon_f}}$$

Where,

$D_{EA}$ = diameter of equivalent annulus of fuel in a unit cell

A vertical cross-section of a unit cell is shown below.

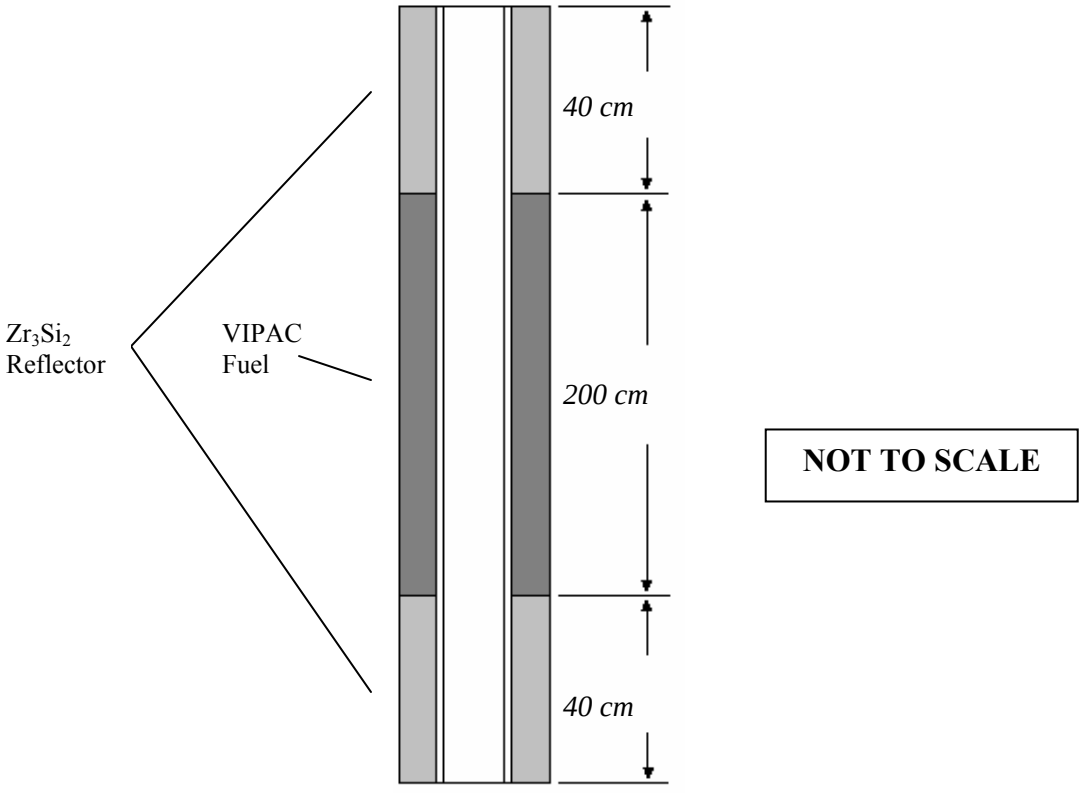


**Fig. A-C.2 Vertical Cross-Section of Unit Cell**

**ODS MA956 Properties**

*Thermal Conductivity*

The temperature-dependent thermal conductivity of unirradiated ODS MA956 cladding is shown in the figure below. [2]

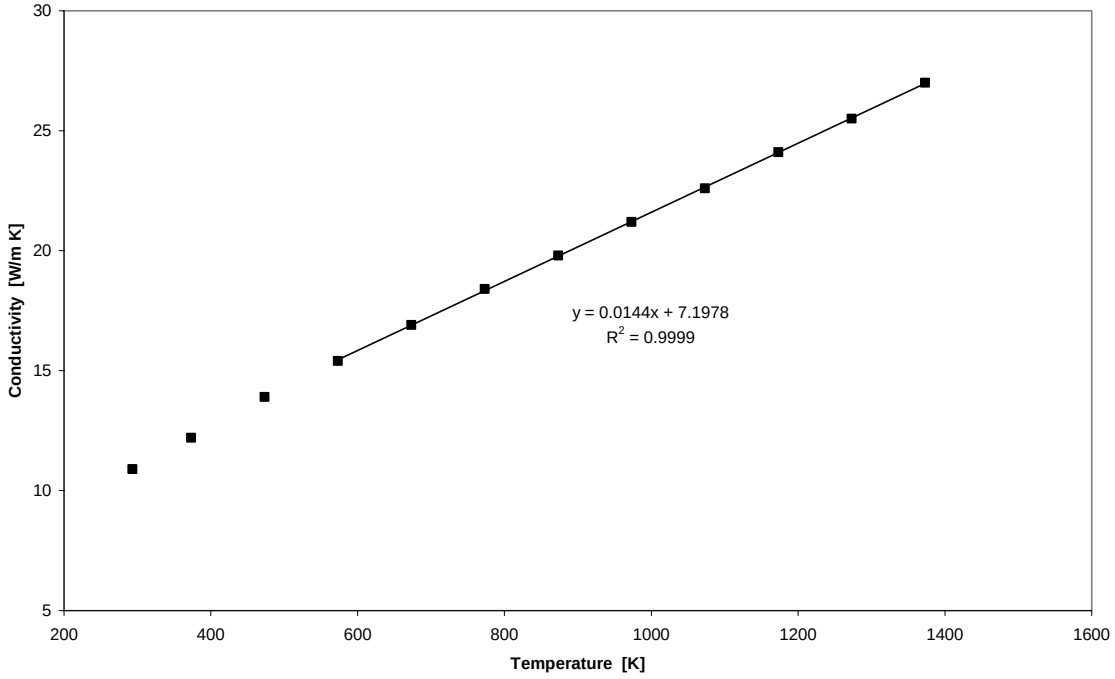


**Fig. A-C.3 Conductivity Versus Temperature for ODS MA956**

$K = 0.0144\ T + 7.1978$

Where
$T$ = temperature in Kelvins
$K$ = Thermal conductivity in W/m K

For the benchmarking exercise, a constant cladding conductivity of 16 W/m·K was assumed.

*Density*

ODS MA956 cladding density is taken to be 7.2 g/cm$^3$

[2] Values of conductivity were taken from Special Metals Corporation, Publication number SMC – 008, 1999. Linear fit using temperatures from 600 K – 1100 K.

**UC VIPAC Fuel Properties**

*Thermal Conductivity*

Assumed a constant conductivity of 15 W/m·K

This is an estimate using the 1500°C value of 17 W/m·K given in [Waltar, et. al., 1981]. Corrected for porosity, we get (0.91)(17 W/m·K) = 15.47. For conservativism, we take the value to be 15 W/m·K. Note that this estimate is quite rough and does not account for irradiation. However, it will suffice for a numerical benchmark.

*Density*

Vipac UC having 91% smear density
$\rho$ = 12.37 g/cm$^3$

**Helium Coolant Properties**

*Thermal conductivity*

Use NIST

*Density*

Can assume ideal gas and thus helium density is given by

$$\rho = \frac{P}{RT} = \frac{P}{\left(2076.9 \frac{J}{kg \cdot K}\right)(T)}$$

Where
$P$ = pressure in Pa
$T$ = temperature in Kelvins
$\rho$ = helium density in kg/m$^3$

So for the channel inlet conditions (420°C and 10 MPa) the density is 6.94 kg/m$^3$.

*Prandtl*

NIST was used here, but can assume Prandtl number to constant and equal to 0.65.

*Heat capacity*

$c_p$ = 5186 J/kg·K

```
**********************************************************************
    * PROGRAM FOR FLOW SPLIT IN PARALLEL NONCOMMUNICATING CHANNELS
          *        PAVEL 1/8/93    UPDATED 12/2004 by POPE
**********************************************************************

                              ---INPUT DATA PRINTOUT---

  === 2400MW TID B&B benchmark core Helium Coolant 1/18/05 ==   EPS  ELT (m)  cosfi   0.10000D-02
0.28000D+01 0.10000D+01
 N1     NZ  ICOOl  NP(I),I=1,N1   (ave,hot)                          2     20      2  59683     61
 D1(I),I=1,N1 - HYDRAULIC DIAMETERS (m)                          0.10000D-01 0.10000D-01
 ICS(I),I=1,N1 - CHANNEL STATUS: 0-SMOOTH,  1-ROUGHNED                 0      0
 ISH(I),I=1,N1 - CHANNEL SHAPE: 1-ROUND,  2-ANNULAR                    1      1
 A1(I),I=1,N1 - FLOW AREAS    (m)                                0.79000D-04 0.79000D-04
 PH1(I),I=1,N1 - HEATED PERIMETER  (m)                           0.31416D-01 0.31416D-01
 EKI(I),I=1,N1 - INLET FORM LOSSES                                0.50000D+00 0.50000D+00
 EKO(I),I=1,N1 - OUTLET FORM LOSSES                               0.10000D+01 0.10000D+01
 DEL(I),I=1,N1 - SURFACE ROUGHNESS                                0.00000D+00 0.00000D+00
 QPPM(I),I=1,N1 - AVERAGE HEAT FLUX -q''av, average and hot (W/m^2)   0.63900D+06 0.11300D+07
 DZ(J),J=1,NZ - NODE LENGTH                                         0.080  0.080  0.080  0.080  0.080
0.200  0.200  0.200  0.200  0.200  0.200  0.200  0.200  0.200  0.200  0.080  0.080  0.080  0.080  0.080
 XSI(J),J=1,NZ - AXIAL DISTRIBUTION OF HEAT FLUX q''(z)/q''av          0.000  0.000  0.000  0.000  0.000
0.455  0.798  1.081  1.282  1.387  1.387  1.282  1.081  0.798  0.455  0.000  0.000  0.000  0.000  0.000
 NGRID IGRID                                                           0      0
 TIN (K)      PIN(Pa)       EMT (kg/s)                          0.69315D+03 0.10000D+08 0.31830D+04
 CLADTH(I), I=1,N1 - CLADDING THICKNESS (m)                       0.80000D-03 0.80000D-03
 REA(I), I=1,N1 - RADIUS OF EQUIVALENT ANNULUS OF FUEL (m)        0.70710D-02 0.70710D-02
                      ***************** END OF INPUT DATA PRINTOUT ****************

                          -----RESULTS------
                      CHANNEL 1    CHANNEL 2   CHANNEL 3    CHANNEL 3+I
 FLOW RATE  (KG/S)     3.1799E+03  3.0496E+00
 PRES.DROP-TOTAL (Pa)  2.3170E+05  2.3187E+05
 FRICTION DP (Pa)      1.6629E+05  1.6338E+05
 Form losses  (Pa)     5.7614E+04  5.6182E+04
 Acceleration DP(Pa)   7.6317E+03  1.2158E+04
 Gravity DP (Pa)       1.6806E+02  1.5628E+02
 HEAT TRANSFER COEF.   9.2121E+03  8.9413E+03
 REYNOLDS NUMBER       1.6497E+05  1.4009E+05
 INLET VELOCITY(M/S)   9.8812E+01  9.2733E+01
 MASS FLUX KG/m2-s     6.7444E+02  6.3295E+02
```

----AXIAL PROFILES IN THE CHANNELS----

| # | Z (m) | Tfluid (C) | Cp (kJ/kg K) | Twal (C) | TCmax (C) | TFmax (C) | X (-) | P (MPa) | ' | h (kW/m2K) | Vel (m/s) | DNBR (-) | q" (MW/m2) | ro (kg/m3) |
|---|---|---|---|---|---|---|---|---|---|---|---|---|---|---|
| CHANNEL # 1 | | | | | | | | | | | | | | |
| 1 | 0.08 | 420.01 | 5.19 | 420.01 | 420.01 | 420.01 | 1.000 | 9.9791 | | 11.71 | 99.02 | 0.00 | 0.00 | 6.81 |
| 2 | 0.16 | 420.01 | 5.19 | 420.01 | 420.01 | 420.01 | 1.000 | 9.9749 | | 10.89 | 99.06 | 0.00 | 0.00 | 6.81 |
| 3 | 0.24 | 420.02 | 5.19 | 420.02 | 420.02 | 420.02 | 1.000 | 9.9707 | | 10.49 | 99.10 | 0.00 | 0.00 | 6.81 |
| 4 | 0.32 | 420.02 | 5.19 | 420.02 | 420.02 | 420.02 | 1.000 | 9.9664 | | 10.24 | 99.14 | 0.00 | 0.00 | 6.80 |
| 5 | 0.40 | 420.02 | 5.19 | 434.46 | 434.46 | 434.46 | 1.000 | 9.9622 | | 10.07 | 99.18 | 0.00 | 0.00 | 6.80 |
| 6 | 0.60 | 426.64 | 5.19 | 467.61 | 481.09 | 491.33 | 1.000 | 9.9512 | | 9.77 | 100.22 | 0.00 | 0.29 | 6.73 |
| 7 | 0.80 | 438.24 | 5.19 | 500.59 | 524.24 | 542.19 | 1.000 | 9.9398 | | 9.63 | 101.96 | 0.00 | 0.51 | 6.61 |
| 8 | 1.00 | 453.95 | 5.19 | 533.40 | 565.44 | 589.76 | 1.000 | 9.9279 | | 9.50 | 104.29 | 0.00 | 0.69 | 6.47 |
| 9 | 1.20 | 472.58 | 5.19 | 562.70 | 600.70 | 629.54 | 1.000 | 9.9155 | | 9.46 | 107.05 | 0.00 | 0.82 | 6.30 |
| 10 | 1.40 | 492.74 | 5.19 | 586.89 | 628.00 | 659.20 | 1.000 | 9.9026 | | 9.41 | 110.03 | 0.00 | 0.89 | 6.13 |
| 11 | 1.60 | 512.90 | 5.19 | 603.89 | 645.00 | 676.20 | 1.000 | 9.8894 | | 9.37 | 113.02 | 0.00 | 0.89 | 5.97 |
| 12 | 1.80 | 531.53 | 5.19 | 612.21 | 650.20 | 679.04 | 1.000 | 9.8758 | | 9.36 | 115.81 | 0.00 | 0.82 | 5.82 |
| 13 | 2.00 | 547.24 | 5.19 | 611.63 | 643.67 | 667.98 | 1.000 | 9.8621 | | 9.32 | 118.20 | 0.00 | 0.69 | 5.71 |
| 14 | 2.20 | 558.84 | 5.19 | 601.89 | 625.55 | 643.49 | 1.000 | 9.8484 | | 9.30 | 120.01 | 0.00 | 0.51 | 5.62 |
| 15 | 2.40 | 565.46 | 5.19 | 581.13 | 594.62 | 604.85 | 1.000 | 9.8348 | | 9.27 | 121.11 | 0.00 | 0.29 | 5.57 |
| 16 | 2.48 | 565.46 | 5.19 | 565.46 | 565.46 | 565.46 | 1.000 | 9.8294 | | 9.26 | 121.18 | 0.00 | 0.00 | 5.57 |
| 17 | 2.56 | 565.46 | 5.19 | 565.46 | 565.46 | 565.46 | 1.000 | 9.8239 | | 9.25 | 121.24 | 0.00 | 0.00 | 5.56 |
| 18 | 2.64 | 565.46 | 5.19 | 565.46 | 565.46 | 565.46 | 1.000 | 9.8185 | | 9.24 | 121.31 | 0.00 | 0.00 | 5.56 |
| 19 | 2.72 | 565.47 | 5.19 | 565.47 | 565.47 | 565.47 | 1.000 | 9.8130 | | 9.22 | 121.38 | 0.00 | 0.00 | 5.56 |
| 20 | 2.80 | 565.47 | 5.19 | 565.47 | 565.47 | 565.47 | 1.000 | 9.8076 | | 9.21 | 121.44 | 0.00 | 0.00 | 5.55 |

CHANNEL # 2----------

| | | | | | | | | | | | | |
|---|---|---|---|---|---|---|---|---|---|---|---|---|
| 1 | 0.08 | 420.01 | 5.19 | 420.01 | 420.01 | 420.01 | 1.000 | 9.9815 | 11.12 | 92.90 | 0.00 | 0.00 | 6.81 |
| 2 | 0.16 | 420.01 | 5.19 | 420.01 | 420.01 | 420.01 | 1.000 | 9.9778 | 10.34 | 92.94 | 0.00 | 0.00 | 6.81 |
| 3 | 0.24 | 420.01 | 5.19 | 420.01 | 420.01 | 420.01 | 1.000 | 9.9740 | 9.96 | 92.97 | 0.00 | 0.00 | 6.81 |
| 4 | 0.32 | 420.02 | 5.19 | 420.02 | 420.02 | 420.02 | 1.000 | 9.9703 | 9.73 | 93.01 | 0.00 | 0.00 | 6.81 |
| 5 | 0.40 | 420.02 | 5.19 | 446.91 | 446.91 | 446.91 | 1.000 | 9.9665 | 9.56 | 93.04 | 0.00 | 0.00 | 6.80 |
| 6 | 0.60 | 432.48 | 5.19 | 508.66 | 532.51 | 550.61 | 1.000 | 9.9564 | 9.29 | 94.78 | 0.00 | 0.51 | 6.68 |
| 7 | 0.80 | 454.33 | 5.19 | 570.10 | 611.93 | 643.67 | 1.000 | 9.9455 | 9.17 | 97.76 | 0.00 | 0.90 | 6.47 |
| 8 | 1.00 | 483.93 | 5.19 | 630.37 | 687.02 | 730.02 | 1.000 | 9.9339 | 9.12 | 101.78 | 0.00 | 1.22 | 6.22 |
| 9 | 1.20 | 519.03 | 5.19 | 685.68 | 752.87 | 803.86 | 1.000 | 9.9214 | 9.05 | 106.54 | 0.00 | 1.45 | 5.94 |
| 10 | 1.40 | 557.01 | 5.19 | 730.38 | 803.08 | 858.25 | 1.000 | 9.9082 | 9.04 | 111.71 | 0.00 | 1.57 | 5.67 |
| 11 | 1.60 | 594.98 | 5.19 | 761.35 | 834.05 | 889.22 | 1.000 | 9.8944 | 9.06 | 116.90 | 0.00 | 1.57 | 5.41 |
| 12 | 1.80 | 630.08 | 5.19 | 777.41 | 844.60 | 895.60 | 1.000 | 9.8801 | 9.06 | 121.73 | 0.00 | 1.45 | 5.20 |
| 13 | 2.00 | 659.67 | 5.19 | 776.89 | 833.55 | 876.55 | 1.000 | 9.8655 | 9.06 | 125.84 | 0.00 | 1.22 | 5.03 |
| 14 | 2.20 | 681.52 | 5.19 | 759.84 | 801.67 | 833.41 | 1.000 | 9.8509 | 9.04 | 128.93 | 0.00 | 0.90 | 4.91 |
| 15 | 2.40 | 693.98 | 5.19 | 722.54 | 746.38 | 764.48 | 1.000 | 9.8364 | 9.00 | 130.78 | 0.00 | 0.51 | 4.84 |
| 16 | 2.48 | 693.98 | 5.19 | 693.98 | 693.98 | 693.98 | 1.000 | 9.8308 | 8.99 | 130.86 | 0.00 | 0.00 | 4.84 |
| 17 | 2.56 | 693.99 | 5.19 | 693.99 | 693.99 | 693.99 | 1.000 | 9.8251 | 8.98 | 130.93 | 0.00 | 0.00 | 4.83 |
| 18 | 2.64 | 693.99 | 5.19 | 693.99 | 693.99 | 693.99 | 1.000 | 9.8194 | 8.96 | 131.01 | 0.00 | 0.00 | 4.83 |
| 19 | 2.72 | 693.99 | 5.19 | 693.99 | 693.99 | 693.99 | 1.000 | 9.8137 | 8.95 | 131.08 | 0.00 | 0.00 | 4.83 |
| 20 | 2.80 | 694.00 | 5.19 | 694.00 | 694.00 | 694.00 | 1.000 | 9.8081 | 8.94 | 131.16 | 0.00 | 0.00 | 4.83 |

---AVERAGE COOLANT DENSITY= 6.17-----

---OUTLET MIXED COOLANT PROPERTIES---

Hex= 4388.72kJ/kg, Xex= 0.000 Tex= 565.59C, ROex= 5.55KG/m3

## Appendix D Heatric™ PCHE With 2:1 Channel Ratio

At their visit to MIT in Fall 2003 the Heatric™ engineers indicated that one could sandwich one fluid channel between two others: e.g.

2:1 Configuration Cell vs. Standard 1:1 cell


Keep channel designated "*b*" $q$, $\dot{m}$, $\Delta T_c$ the same.

Then for Case I, each "a" channel at same $\Delta T_c$ has a lower $\dot{m}$ by a factor of 2, and since $\Delta P \approx \dot{m}^2$, pressure drop is lower by a factor of 4.

Furthermore, per channel, work $W \approx \frac{\dot{m}}{\rho} \Delta P$, hence lower by factor of 8; but there are 2 channels, hence $W_{TOTAL}$ is lower by 4 times.

One also has $q = hA_s\Delta T_f$ where $A_s$ = surface area per channel ≡ same.

In laminar flow h is the same, hence $\Delta T_f$ is lower by a factor of 2.

In turbulent flow $h \approx (\mathrm{Re})^{0.8} \approx \mathrm{Re}^{1.0} \approx \dot{m}$, thus h is lower by a factor of 2, which makes $\Delta T_f$ the same.

This type of configuration could be of use when the primary and secondary sides contain fluids of significantly different thermal-hydraulic properties and/or one wants to reduce circulator work on the primary side of an IHX. Of course the IHX increases in size by ≈1.5x. For liquids on the primary side one could use a 2 channel secondary to reduce $CO_2$ pressure drop and thereby increase cycle efficiency.

## Appendix E GFR Project Publications

### Bibliography of MIT GFR Publications

In the interest of completeness, this list includes all topical reports, journal publications and meeting transactions published as a product of the following five coordinated GFR projects at MIT:

- LDRD from INEEL on innovative GFR design: the subject of this final report
- INERI with ANL/CEA etc. on GFR, with MIT focus on shutdown heat removal (continuing)
- NERI from DOE on breed and burn core concept (continuing)
- GEN-IV via INEEL on materials evaluation (ended on 3/31/04)
- GEN-IV via Sandia on supercritical $CO_2$ Brayton cycle assessment (continuing)

This compilation does not include the monthly/quarterly/annual reports routinely generated in the course of these projects. The information in such reports is, in general, published in a more complete and thoroughly interpreted form in the reports listed here.

Those publications preceded by an asterisk (*) are attributed in toto or primarily to the subject LDRD rather than to its subsequent spin-offs.

### Conference Transactions and Journal Articles


1. P. Hejzlar, M. J. Driscoll and N. E. Todreas, **A Modular Gas Turbine Fast Reactor Concept** (MFGR-GT), Transactions of the American Nuclear Society, Vol. 84, p.242, Milwaukee, June 17-21, 2001
2. V. Dostal, P. Hejzlar, M.J. Driscoll, and N.E. Todreas, **A Supercritical $CO_2$ Brayton Cycle for Advanced Reactor Applications**, Transactions of the American Nuclear Society, Vol. 85, p.110, Reno, Nevada, November 11-15, 2001
3. K. Yu, M.J. Driscoll, and P. Hejzlar, **Neutronic Limits of Breed and Burn Fast Reactor Performance**, Transactions of the American Nuclear Society, Vol. 86, p.335-336, Hollywood, Florida, June 9-13, 2002.
4. M.J. Driscoll, P. Hejzlar, and N.E. Todreas, **Fuel-In-Thimble GCFR Concepts for GEN-IV Service**, International Congress on Advanced Nuclear Power Plants, Hollywood, Florida, June 9-13, 2002.
5. P. Hejzlar, M.J. Driscoll, and N.E. Todreas, **The Long-Life Gas Turbine Fast Reactor Matrix Core Concept**, International Congress on Advanced Nuclear Power Plants, Hollywood, Florida, June 9-13, 2002
6. Y. Okano, P. Hejzlar, N.E. Todreas, and M.J. Driscoll, **Thermal-Hydraulics and Post-Shutdown Cooling of a $CO_2$ -Cooled, Gas Turbine Fast Reactor**, Transactions of the American Nuclear Society, Vol. 86, p.139-141, Hollywood, Florida, June 9-13, 2002.

7. V. Dostal, P. Hejzlar, M.J. Driscoll, and N.E. Todreas, **A Supercritical $CO_2$ Gas Turbine Power Cycle for Next Generation Nuclear Reactors**, ICONE 10-22192, 10th International Conference on Nuclear Engineering, Arlington, Virginia, April 14-18, 2002.
8. K. Yu, M.J. Driscoll, and P. Hejzlar, **Neutronic Screening of Diluents for GCFR Fuel**, Transactions of the American Nuclear Society, Vol. 87, p.386-387, Washington, D.C., November 17-21, 2002.
9. V. Dostal, P. Hejzlar, M.J. Driscoll and N.E. Todreas, **Component Design for a Supercritical $CO_2$ Brayton Cycle**, Transactions of the American Nuclear Society, Vol. 87, p.536-537, Washington, D.C., November 17-21, 2002.
10. V. Dostal, P. Hejzlar, M.J. Driscoll and N.E. Todreas, **Realism in Brayton Cycle Calculations**, Transactions of the American Nuclear Society, Vol. 87, p.534-535, Washington, D.C., November 17-21, 2002.
11. K. Yu M. J. Driscoll, P. J. Yarsky, M. A. Pope and P. Hejzlar, **Comparison of GFR Core Reflectors**, Transactions of the American Nuclear Society, Vol. 88, p.520-523, San Diego CA, June 1-5, 2003
12. M. J Driscoll. and P. Hejzlar, **Active or Passive Post-LOCA Cooling of GFRs?**, Transactions of the American Nuclear Society, Vol. 88, p.673-677, San Diego CA, June 1-5, 2003
13. M. J. Driscoll, P. Hejzlar, K. D Weaver. and M. K. Meyer, **Basic Design Choices for a Breed and Burn Fast Reactor**, Transactions of the American Nuclear Society, Vol. 88, p.678-680, San Diego CA, June 1-5, 2003
14. W-J. Lee, B-D. Chung, Y-J. Lee, J-H. Chang, P. Hejzlar, M.J. Driscoll, **Development of MARS-GCR for Gas Cooled Reactor Analysis - Incorporation of Gas Properties** The 10th International Topical Meeting on Nuclear Reactor Thermal Hydraulics (NURETH-10) Seoul, Korea, October 5-11, 2003
15. M.A. Pope, M.J. Driscoll, P. Hejzlar, **Reactor Physics Studies in Support of GFR Core Design**, Transactions of the American Nuclear Society, Proceedings of GLOBAL '03, New Orleans, LA, Nov. 16-21, 2003
16. M.J. Driscoll, M.A. Pope, P. Hejzlar, **Device for Passive Reactivity Insertion During GFR LOCA**, Transactions of the American Nuclear Society, 2003 Winter Meeting, Vol. 89, p.578-579, New Orleans, LA, Nov. 16-21, 2003
17. M.J. Driscoll, M.A. Pope, P. Hejzlar, **Self-Actuated Reactivity Insertion Device for GFR Service**, Transactions of the American Nuclear Society, 2003 Winter Meeting, Vol. 89, p.573-575, New Orleans, LA, Nov. 16-21, 2003
18. N.A. Carstens, M.J. Driscoll, **LOCA-Powered SCRAM Device for GFRs**, Transactions of the American Nuclear Society, 2003 Winter Meeting, Vol. 89, p.576-577, New Orleans, LA, Nov. 16-21, 2003

19. Y. Wang, V. Dostal, P. Hejzlar, **Turbine Design for Supercritical $CO_2$ Brayton Cycle**, Transactions of the American Nuclear Society, Vol, 89, Proceedings of GLOBAL '03, New Orleans, LA, Nov. 16-21, 2003
20. W. Williams, P. Hejzlar, P. Saha, **Analysis of a Convection Loop for GFR Post-LOCA Decay Heat Removal**, Proceedings of ICONE 12, April 25-29, Arlington, VA, 2004
21. M.J. Delaney, G.E. Apostolakis, **A Probabilistic Analysis of General Design Criterion 35 for a Gas-Cooled Fast Reactor**, Proceedings of ICAPP '04, Pittsburgh, PA, Vol. 90, June 13-17, 2004
22. W. Williams, P. Hejzlar, M.J. Driscoll, **Decay Heat Removal from a GFR Core by Natural Convection**, Proceedings of ICAPP '04, Pittsburgh, PA, Vol. 90, June 13-17, 2004
23. P. Yarsky, M.J. Driscoll, P. Hejzlar, **Neutronic Studies of Nuclear Fuels for a Breed and Burn GFR**, Proceedings of ICAPP '04, Pittsburgh, PA, June 13-17, 2004
24. P. Yarsky, M.J. Driscoll, P. Hejzlar, **Use of Minimally Processed Fast Reactor Fuel in Light Water Reactors**, Trans. Am. Nucl. Soc., Pittsburgh, PA, Vol. 90, June 13-17, 2004
25. M.J. Driscoll, P. Hejzlar, M. J. Delaney, W. C. Williams, C. Matos, **Compressed Gas Emergency Power Supply for GFR Service**, Trans. Am. Nucl. Soc., Pittsburgh, PA, Vol. 90, June 13-17, 2004
26. V. Dostal, M.J. Driscoll, P. Hejzlar, Y. Wang, **Supercritical $CO_2$ Cycle for Fast Gas-Cooled Reactors**, Proc. of ASME TurboExpo, Vienna, Austria, June, 2004
27. Y. Wang, G. Guenette, P. Hejzar, M.J. Driscoll, **Compressor Design for the Supercritical $CO_2$ Brayton Cycle**, Proc. of 2nd Int. Energy Conversion Conference, 16-19 Aug. 2004, Providence, RI

**CANES MIT-ANP-TR and PR Series**

1. M. J. Driscoll, P. Hejzlar, N. E. Todreas, Y. Okano, V. Dostal and K. Yu, **Development of Gen IV Advanced Gas-Cooled Reactors with Hardened/Fast Neutron Spectrum**, Annual Progress Report, MIT-ANP-PR-093, September 2002
2. K. Yu, M.J. Driscoll, and P. Hejzlar, **Neutronic Evaluation of GCFR Core Diluents**, MIT-ANP-TR-086, June 2003
3. M. J. Driscoll, P. Hejzlar, N.E. Todreas, and B. Veto, **Modern GCFR Safety Assurance Considerations**, MIT-ANP-TR-087, May 2003
4. Y. Okano, P. Hejzlar, N.E. Todreas, and M.J. Driscoll, **Thermal Hydraulics and Shutdown Cooling of Supercritical $CO_2$ GT-GCFRs**, MIT-ANP-TR-088, August 2002

5. V. Dostal, M.J. Driscoll, P. Hejzlar, and N.E. Todreas, **$CO_2$ Brayton Cycle Design and Optimization** MIT-ANP-TR-090, November 2002
6. W. Williams, P. Hejzlar, M.J. Driscoll, W-J. Lee, and P. Saha, **Analysis of A Convection Loop for GFR Post - LOCA Decay Heat Removal from a Block-Type Core**, MIT-ANP-TR-095, March 2003
7. V. Dostal, M.J. Driscoll, P. Hejzlar, **A Supercritical Carbon Dioxide Cycle for Next Generation Reactors,** MIT-ANP-TR-100, March 10, 2004
8. K. Gezelius, **Design of Compact Intermediate Heat Exchangers for Gas Cooled Fast Reactors**, MIT-ANP-TR-103, June 2004
9. M.A. Pope, M. Driscoll, P. Hejzlar, **Reactor Physics Design of Supercritical $CO_2$ – Cooled Fast Reactors,** MIT-ANP-TR-104, September 2004

**GFR Series, MIT-GFR-001 to MIT-GFR-019**

1. S. Thon, **Selection of Materials for a Supercritical $CO_2$ Cooled GCFR,** MIT-GFR-001, Aug. 2002
2. J. Eapen, **Analysis of a Natural Convection Loop for Post-LOCA GCFR Decay Heat Removal,** MIT-GFR-002, Dec. 2002
3. Y. Wang, **Aerodynamic Design of Turbine for S-$CO_2$ Brayton Cycle,** MIT-GFR-003, June 2003
4. K. Gezelius, V. Dostal, M.J. Driscoll, P. Hejzlar, **Design of Shell and Tube Heat Exchanger for the S-$CO_2$ Cycle and Laminar Flow in Microchannel Heat Exchangers,** MIT-GFR-004, May 2003
5. P. Yarsky, **Neutronic Evaluation of GFR Breed and Burn Fuels,** MIT-GFR-005, May 2003
6. L. B. Fishkin **,Use of the Prestressed Cast Iron Vessel in Nuclear Reactor Applications,** MIT-GFR-006, April 2004
7. J. Plaue, K.R. Czerwinski, **Evaluation of Uranium Carbide and Sulfide Fuels for a Gas-Cooled Fast Reactor Utilizing Dry Reprocessing,** MIT-GFR-007, October 2003
8. M.J. Delaney, C. Matos, B.T. Parks, J.P. Koser, Interim Report on Task 1**, GFR PRA-Guided Plant Design and Core Materials Compatibility Studies for $CO_2$ Cooled Reactor,** Annual Report on Project: Plant Design and Core Materials Compatibility Studies for Supercritical $CO_2$ Cooled Reactors, MIT-GFR-008, March 2004
9. W. Williams, P. Hejzlar, P. Saha, M.J. Driscoll, **Comparative Analysis of Decay Heat Removal Approaches for a Block GFR Core** MIT-GFR-009

10. D. Rigual, P. Stahle, Y. Ostrovsky, Y.H. Jeong, R. Ballinger, Interim Report on Task 2: **Loops for Corrosion Tests in Supercritical $CO_2$ in the Presence of Radiolysis**, Annual Report on Project: Plant Design and Core Materials Compatibility Studies for Supercritical $CO_2$ Cooled Reactors**,** MIT-GFR-010, March 2004
11. J. Plaue, K. Czerwinski, Interim Report on Task 3: **Fuel Material Interactions,** Annual Report on Project: Plant Design and Core Materials Compatibility Studies for Supercritical $CO_2$ Cooled Reactors**,** MIT-GFR-011, March 2004
12. Yong Wang, V. Dostal, M.J. Driscoll, P. Hejzlar G.R. Guenette, **Qualification of the Supercritical $CO_2$ Power Conversion Cycle for Advanced Reactor Applications**, Annual / Topical Technical Progress Report, MIT-GFR-012, April 04
13. M. Delaney, G.E. Apostolakis, M.J. Driscoll, **Risk-Informed Design Guidance for a Generation-IV Gas-Cooled Fast Reactor Emergency Core Cooling System,** MIT-GFR-013, May 2004
14. M. J. Driscoll, P. Hejzlar, **300 MWe Supercritical $CO_2$Plant Layout and Design,** MIT-GFR-014, June 2004
15. Yong Wang , G.R. Guenette , P. Hejzlar , M.J. Driscoll , **Supercritical $CO_2$ , Turbine And Compressor Design,** MIT-GFR-015, June 2004
16. Jonatan Hejzlar, **Computer Code for the Analysis of Printed Circuit Heat Exchangers with Zigzag Channels**, MIT-GFR-016, August 2004
17. M.J. Driscoll, P. Hejzlar, N. Carstens, Yong Wang, Interim Topical Report, **Simulation of Supercritical $CO_2$ Brayton Cycle Plants**, MIT-Sandia Report, MIT-GFR-017, Sept. 2004
18. Yong Wang, M.J. Driscoll, P. Hejzlar, G. R. Guenette Interim Topical Report, **Small Scale Supercritical $CO_2$ Components and System for Laboratory Tests,** MIT-Sandia Project, MIT-GFR-018, Sept. 2004
19. M.J. Driscoll**, Interim Topical Report, Supercritical $CO_2$ Plant Cost Assessment,** MIT-Sandia Project, MIT-GFR-019, Sept. 2004
20. P. Stahle, J. Lee, P. Saha, P. Hejzlar, Annual Report, **Design Of Thermal-Hydraulic Loop related to Advanced Gas-Cooled Reactor**, MIT-GFR-020, Oct. 2004
21. M.J. Driscoll, P. Hejzlar, Final Report on LDRD Project, **An Innovative Gas-Cooled Fast Reactor**, MIT-GFR-021 Sept. 2004

**GFR Theses**

1. Jonathan Plaue, **Evaluation of Uranium Carbide and Sulfide Fuels for a Gas-Cooled Fast Reactor Utilizing Dry Reprocessing**, MSC Thesis, MIT Nucl. Eng. Dept., SM-22, June 2003
2. Kun Yu, **Neutronic Evaluation of GCFR Core Diluents and Reflectors**, MSc Thesis, MIT Nucl. Eng. Dept., SM-22, July, 2003

3. Vacek Dostal, **A Supercritical Carbon Dioxide Cycle for Next Generation Reactors,** ScD Thesis, MIT Nucl. Eng. Dept., January 2004
4. Knut Gezelius, **Design of Compact Intermediate Heat Exchangers for Gas Cooled Fast Reactors**, SM/SB Thesis, MIT Nucl. Eng. Dept., May 2004
5. Michael Pope. **Reactor Physics Design of Supercritical $CO_2$ –Cooled Fast Reactors,** SM Thesis, MIT Nucl. Eng. Dept., September 2004

**Dual Publication**

In general theses are also issued separately as topical reports having substantially the same, if not identical content.

The following key identifies these twin publications:

| **Report** | **Thesis Version** |
|---|---|
| MIT-ANP-TR-086 | SM Thesis by Kun Yu |
| MIT-ANP-TR-100 | ScD Thesis by V. Dostal |
| MIT-ANP-TR-103 | SM/SB Thesis by K. Gezelius |
| MIT-ANP-TR-104 | SM Thesis by M.A. Pope |
| MIT-GFR-007 | SM Thesis by J. Plaue |

**Task Flowchart**

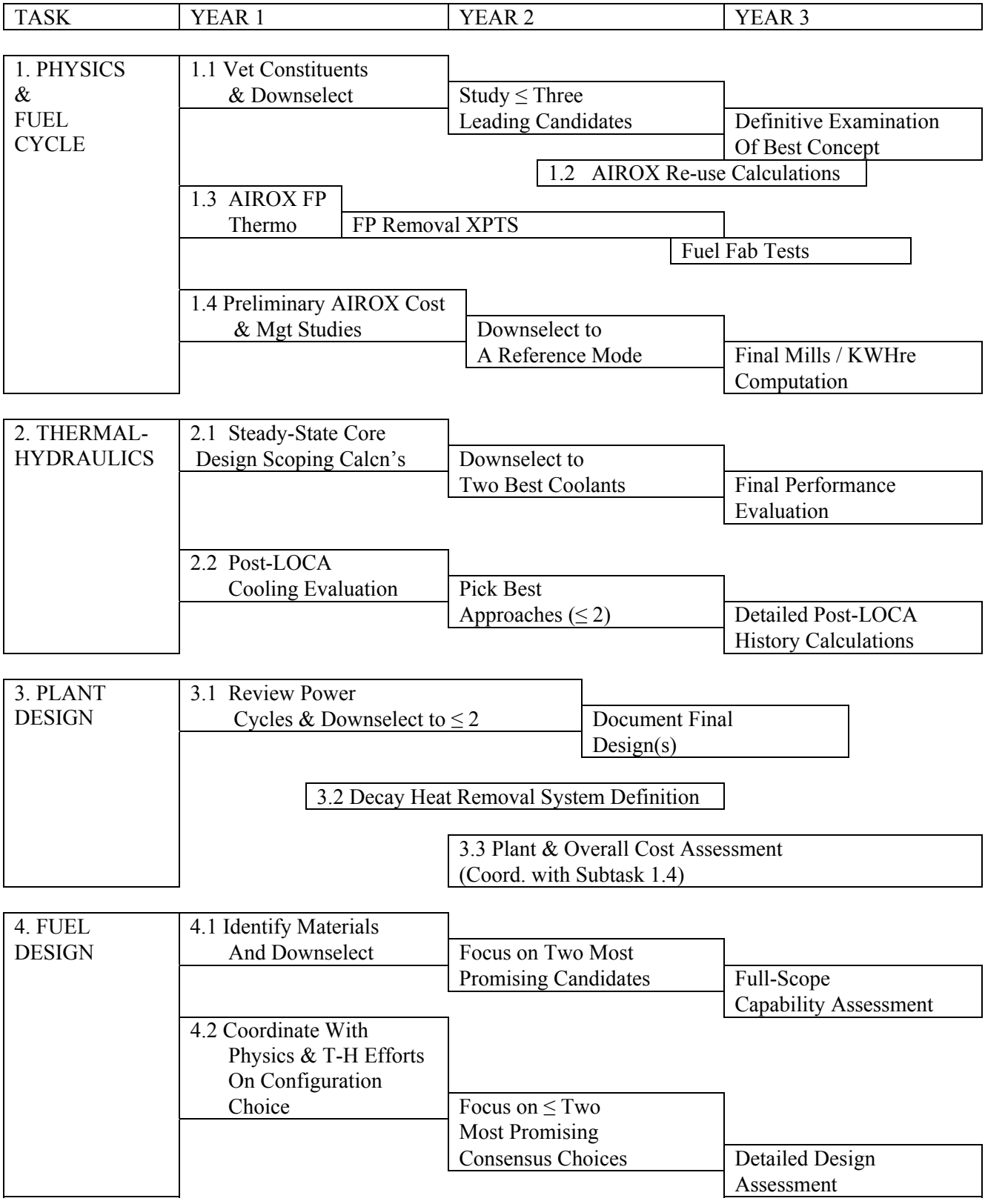

**Milestone Status Table**
**As of 12.31.04**

| Task ID No. | Description | Planned Completion | Actual Completion | Comments |
|---|---|---|---|---|
| 1.1 | • Vet Core Constituents & Downselect<br>• Study Leading Candidates | 9/30/03<br>9/30/04 | 9/30/03<br>9/30/04 | UC and UN-15 are focus |
| 1.3 | • AIROX Thermodynamics<br>• Fission Product Removal Experiments | 7/31/03<br>9/30/04 | 7/31/03<br>Lab Transferred to UNLV; Work Reprogrammed, See Main Text | |
| 1.4 | • AIROX Studies<br>• Select Ref. Mode | 9/30/03<br>9/30/04 | 9/30/03<br>9/30/04 | GFR spent fuel is suitable PWR reload: as $UO_2$ in LWR as UC in GFR |
| 2.1 | • T-H Scoping Studies<br>• Downselect Coolant | 9/30/03<br>9/30/04 | 9/30/03<br>9/30/04 | Indirect, He<br>Primary |
| 2.2 | • Post-LOCA Cooling Evaluations<br>• Pick Best Approach | 9/30/03<br>9/30/04 | 9/30/03<br>9/30/04 | Active Loops With Passive Capability |
| 3.1 | • Review Power Cycles<br>• Downselect Final Design | 6/30/04<br>6/30/05 | 6/30/04<br>12/31/04 | $H_2O$<br>Rankine |
| 3.2 | • Decay Heat Removal System Definition | 9/30/04 | 9/30/04 | Multiloop, Active |
| 3.3 | • Plant and Overall Cost Assessment | 9/30/05 | -- | Using GCRA MHTGR Basis |
| 4.1 | • Identify Materials<br>• Focus on Most Promising | 9/30/03<br>9/30/04 | 9/30/03<br>9/30/04 | UC, UN-15, ODS |
| 4.2 | • Coordinate on Config. Choice<br>• Focus on Most Promising | 9/30/03<br>9/30/04 | 9/30/03<br>9/30/04 | Pin & Tube-in-Duct Vented |

***Notes:*** ***See Preceding Task Flowchart for Newly Initiated Year 3 Tasks for 9/30/05 Completion.***

## Financial Reports

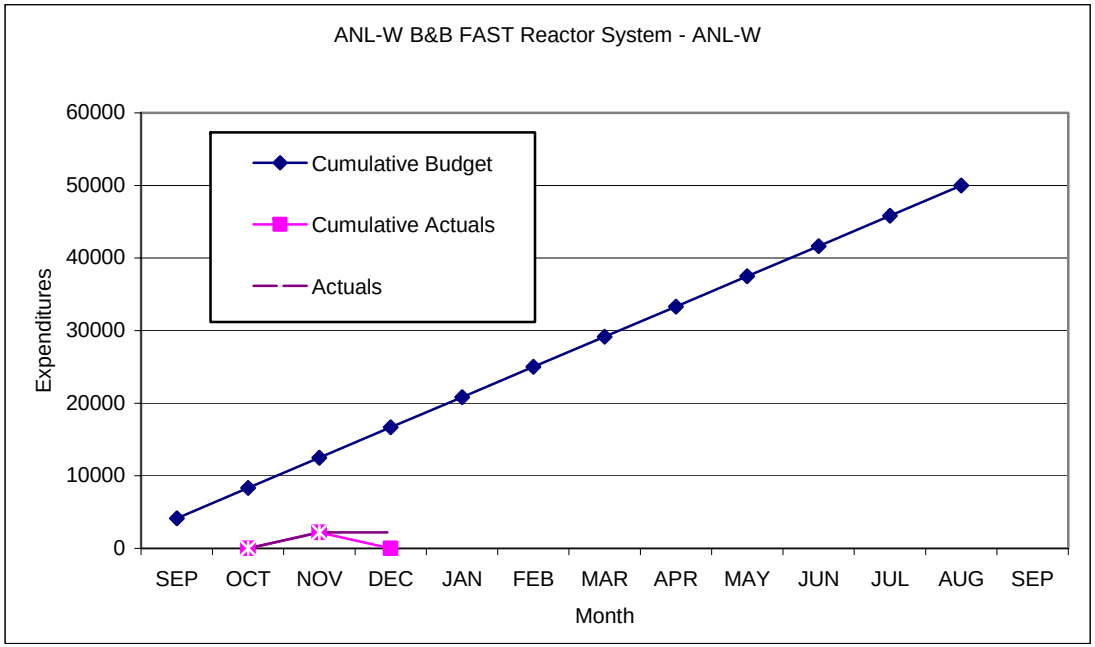


| | SEP | OCT | NOV | DEC | JAN | FEB | MAR | APR | MAY | JUN | JUL | AUG | SEP |
|---|---|---|---|---|---|---|---|---|---|---|---|---|---|
| Cumulative Budget | 4166 | 8332 | 12498 | 16664 | 20830 | 24996 | 29162 | 33328 | 37494 | 41660 | 45826 | 49992 | |
| Cumulative Actuals | | 0 | 2212 | 0 | | | | | | | | | |
| | | | | | | | | | | | | | |
| Budget | 4166 | 4166 | 4166 | 4166 | 4166 | 4166 | 4166 | 4166 | 4166 | 4166 | 4166 | 4166 | |
| Actuals | | 0 | 2212 | 2212 | | | | | | | | | |

**DRISCOLL NERI CONTRACT DE-FG07-02SF22608**
**FY 2004 QUARTERLY FINANCIAL REPORT--MIT PORTION**

***Financial Performance:***

**Quarterly Expenditure Summary:**

| | Totals | Oct | Nov | De | 2003 Jan | Feb | Mar | Apr | May | Jun | Jul | Aug | Sep | Oct | Nov | Dec | 2004 Jan | Feb | Mar | Apr | May | Jun | Jul | Aug | Sep | Oct | Nov | Dec |
|---|---|---|---|---|---|---|---|---|---|---|---|---|---|---|---|---|---|---|---|---|---|---|---|---|---|---|---|---|
| **Monthly Cost** | | | | | | | | | | | | | | | | | | | | | | | | | | | | |
| - Plan | 0 | 25 | 25 | 25 | 25 | 25 | 25 | 25 | 25 | 25 | 25 | 25 | 25 | 25 | 25 | 25 | 25 | 25 | 25 | 25 | 25 | 25 | 25 | 25 | 25 | 25 | 25 | 25 |
| - Actual | 7 | 13 | 24 | 43 | 31 | 30 | 35 | 32 | 23 | 6 | 16 | 13 | 9 | 27 | 21 | 28 | 20 | 14 | 15 | 17 | 18 | 30 | 20 | 21 | 6 | 53 | 10 | 23 |
| **Cumulative** | | | | | | | | | | | | | | | | | | | | | | | | | | | | |
| - Plan | 0 | 25 | 50 | 75 | 100 | 125 | 150 | 175 | 200 | 225 | 250 | 275 | 300 | 325 | 350 | 375 | 400 | 425 | 450 | 475 | 500 | 525 | 550 | 575 | 600 | 625 | 650 | 675 |
| - Actual | 7 | 20 | 44 | 87 | 118 | 148 | 184 | 215 | 239 | 246 | 262 | 275 | 284 | 311 | 332 | 359 | 378 | 393 | 408 | 425 | 443 | 473 | 493 | 514 | 520 | 573 | 583 | 606 |

Note: all numbers are in thousands of dollars.

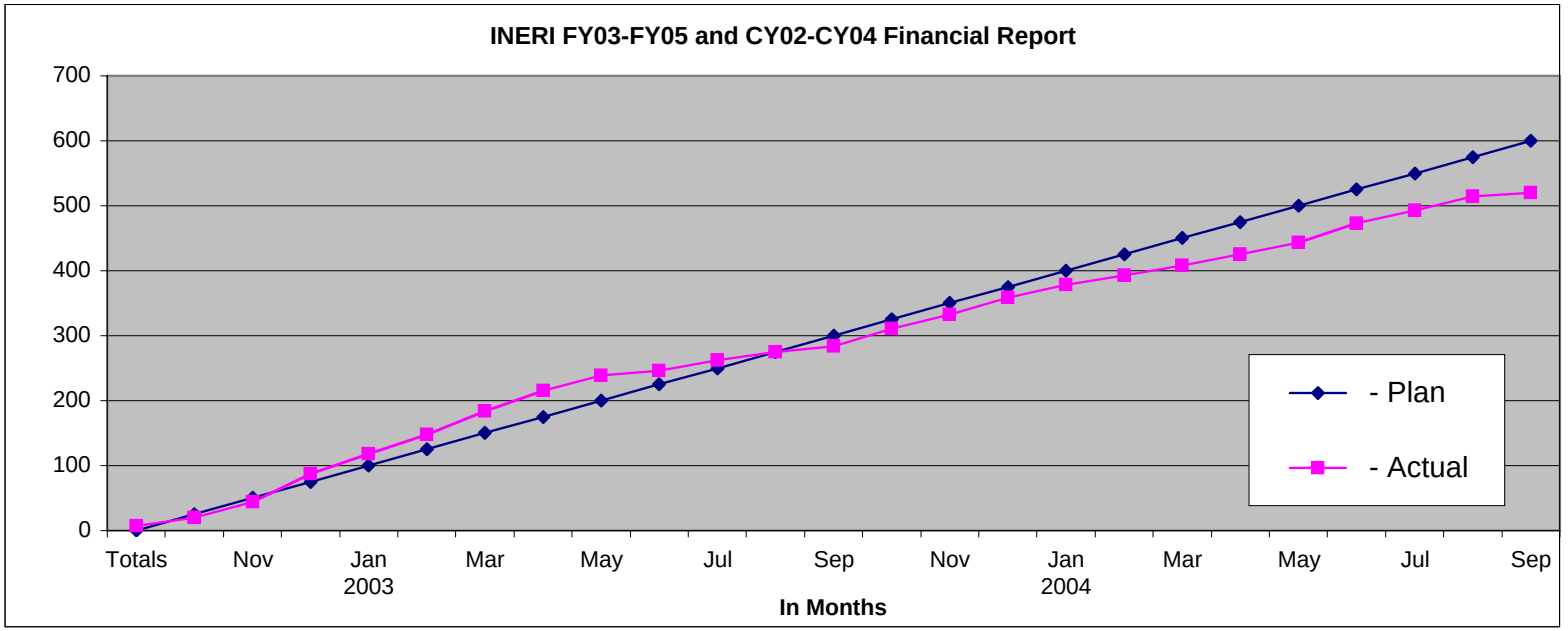

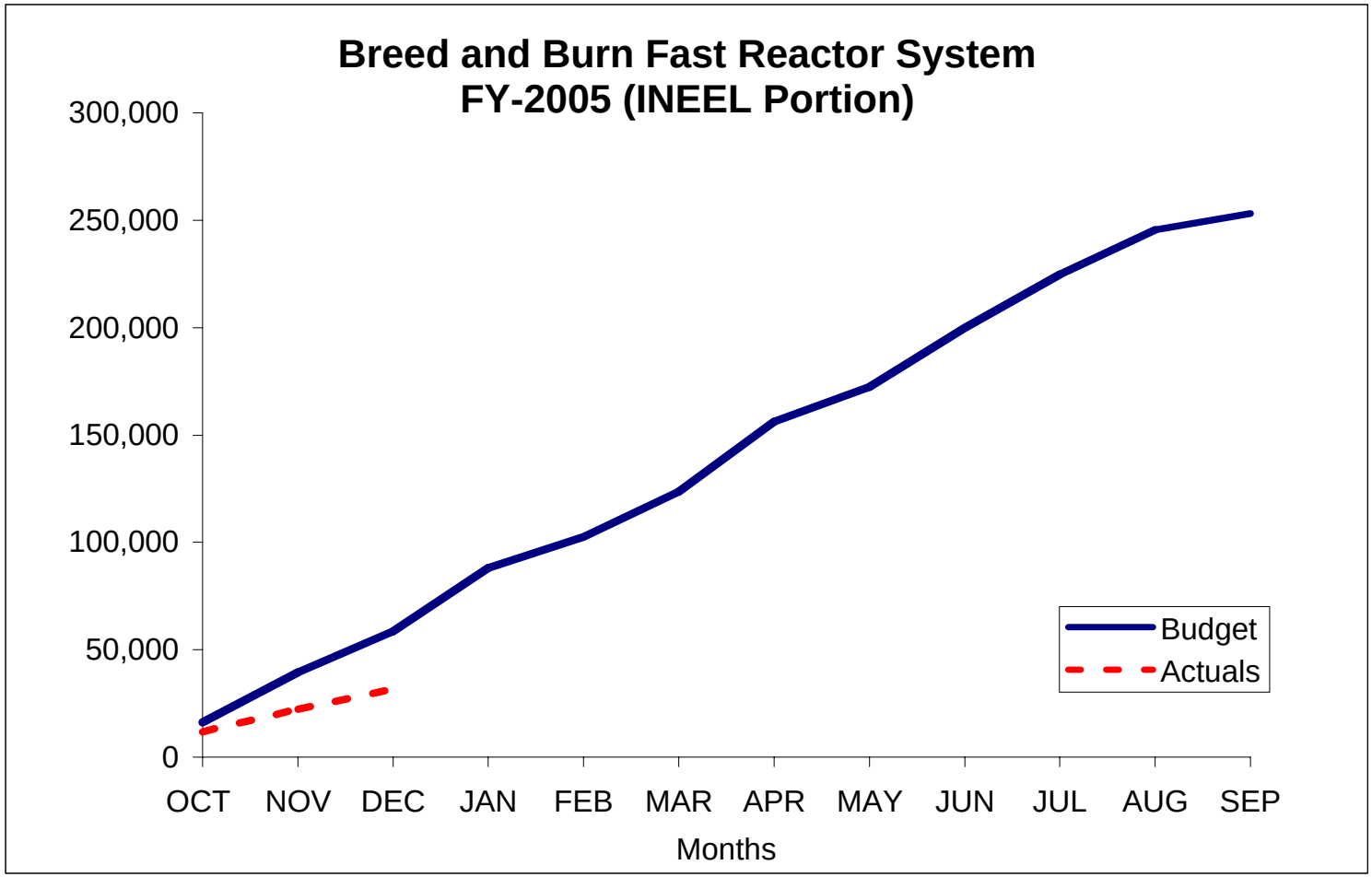


| | OCT | NOV | DEC | JAN | FEB | MAR | APR | MAY | JUN | JUL | AUG | SEP |
|---|---|---|---|---|---|---|---|---|---|---|---|---|
| Budget | 16,274 | 23,313 | 19,103 | 29,417 | 14,521 | 21,057 | 32,556 | 16,233 | 27,485 | 24,770 | 20,719 | 7,580 |
| Actuals | 11,725 | 10,719 | 9,163 | 0 | 0 | 0 | 0 | 0 | 0 | 0 | 0 | 0 |

Cum

| | | | | | | | | | | | | |
|---|---|---|---|---|---|---|---|---|---|---|---|---|
| Budget | 16,274 | 39,587 | 58,690 | 88,107 | 102,628 | 123,685 | 156,241 | 172,474 | 199,959 | 224,729 | 245,448 | 253,028 |
| Actuals | 11,725 | 22,444 | 31,607 | | | | | | | | | |

**6893961 Distribution List—Neri B&B**

hejzlar@mit.edu, yarsky@mit.edu, mitchell.meyer@anl.gov, mickeyd@mit.edu, dan.wachs@anlw.anl.gov, weavkd@inel.gov, czerwin2@unlv.nevada.edu, plaue@cmt.anl.gov, bnz@inel.gov, mapope@mit.edu, cbd@inel.gov, psdrept@id.doe.gov, mmartinez@energetics.com, osbornkk@id.doe.gov, 241user@osti.gov, neri@hq.doe.gov, tycwei@anl.gov, buzz.savage@hq.doe.gov, marstd@inel.gov, lynn.hall@hq.doe.gov. **Also, important-submit online through weblink: https://www.osti.gov/elink-241356**

(Pavel Hejzlar, Pete Yasky, Mitch Meyer, Mike Driscoll, Dan Wachs, Kevan Weaver, Ken Czerwinski, Jon Plaue, Jim Sterbentz, Mike Pope, Cliff Davis, PSDREPT, DOE: Marty Martinez, Kenny Osborne and 241 user, neri@hg—GOV ADMIN, Tom Wei, Buzz Savage, marstd—gov admin, Lynn Hall, DOE Office of Scientific and Technical Information